

SEP 17 1987

ORNL
MASTER COPY

ORNL/GCR-87/4

Contract No. DE-AC05-84OR21400

THE FIRST WATER VAPOR INJECTION TESTS IN HFR-B1

B. F. Myers
(Presently on Assignment to ORNL)

August 1987

Oak Ridge National Laboratory
Oak Ridge, Tennessee 37831
operated by
MARTIN MARIETTA ENERGY SYSTEMS, INC.
for the
U.S. Department of Energy

CONTENTS

1. INTRODUCTION	1-1
2. THE FIRST WATER VAPOR INJECTION TESTS IN HFR-B1	2-1
2.1. The Injection and Discharge of Water Vapor	2-1
2.2. The Hydrolysis of Carbonaceous Material	2-9
2.3. The Hydrolysis of the Fuel UCO	2-16
2.4. The Source of the H ₂ and CO	2-28
3. THE FAILURE OF THE DESIGNED-TO-FAIL PARTICLES	3-1
4. TRANSPORT OF GAS FROM CAPSULE TO SAMPLING VOLUME	4-1
4.1. Introduction	4-1
4.2. Analysis of the Gas Train	4-4
4.3. Application of Analysis to the HFR-B1 Measurements	4-7
5. THE DETERMINATION OF HYDROLYSIS PRODUCT CONCENTRATIONS FROM GAS CHROMATOGRAPHIC MEASUREMENTS ON SAMPLES OF OUTLET GAS FROM CAPSULE C	5-1
6. A SELF-TUTORIAL IN GAMMA SPECTROSCOPY	6-1
6.1. Introduction	6-1
6.2. Derivation of Expression for Number Density of Isotope in Sampling Volume at Moment of Collection	6-1
6.3. Total Count Rates and Pulse Pileup Loss Corrections	6-3
6.4. Ratio of Atoms Among Isotopes Measured	6-6

CONTENTS (Continued)

7.	THE DETERMINATION OF R/B, COMPARISON WITH REPORTED VALUES AND DEPENDENCE ON DECAY CONSTANT (PARTIALLY A SELF-TUTORIAL)	7-1
7.1.	Determination of R/B and Comparisons	7-1
7.2.	The Dependence of R/B or Relative R/Bs on Decay Constant	7-2
8.	DETERMINATION OF RELATIVE R/B VALUES FOR ^{85m}Kr FROM MEASUREMENTS DURING THE FIRST WATER VAPOR INJECTION TEST	8-1
9.	RAW DATA ON GAMMA COUNTING OF GAS SAMPLES BETWEEN JUNE 10 AND 20 FROM CAPSULE C	9-1
10.	QUESTIONS, COMMENTS, AND REQUESTS	10-1

FIGURES

2-1.	The water vapor - time profiles in the gas outflow from capsule C	2-4
2-2.	Time profiles of water vapor in outlet gas from capsule C following termination of water vapor injection	2-8
2-3.	Time profiles of H_2 , CO, CO_2 , and water vapor in capsule C	2-13
2-4.	Concentrations of H_2 and CO and time profile of water vapor in capsule C effluent for the second water vapor injection	2-18
2-5.	Time profiles of R/B for ^{85m}Kr and water vapor discharge for the first water vapor injection test	2-23
2-6.	Time profiles of R/B for ^{85m}Kr and water vapor discharge for the second water vapor injection test	2-27
3-1.	Time profiles of R/B values for capsule A, B, and C during the period when the designed-to-fail particles were failing: cycle 87.03 (R/B values are based on total fissile loading)	3-2
3-2.	The cumulative number of particles (dtf) failure as a function of time from start of irradiation	3-6
4-1.	Gas scheme of irradiation rig including rig head (taken from P/F1/87/5)	4-2

FIGURES (Continued)

5-1.	Gas chromatograms in the vicinity of the CO peaks	5-6
5-2.	Examples of the interference by neon in the chromatographic measurement of hydrogen	5-11
5-3.	Example of GC integration variation	5-13
5-4.	Repeated measurement by gas chromatography of the same gas sample	5-14
6-1.	The count- and delay-time corrected number of accumulated counts	6-7
7-1.	Point-source, full-energy peak detection efficiency as a function of gamma-ray energy for five source-detector geometries of the IMGA system	7-5
7-2.	Comparison of relative R/B values from capsule C of HFR-B1 (taken 6/15/87 at 1105: spectrum 2349) with R/B values from Cell 3 of R2-K13	7-8
7-3.	The dependence of R/B on decay constant for fission gas release from capsules A and B before failure of dtf particles	7-11
8-1.	Correlation between t_c and t_d Used to estimate t_c which was missing for spectrum 2399	8-3

TABLES

2-1.	Water vapor level in the outlet gas from capsule C before, during, and after the first two water vapor injection tests	2-2
2-2.	The concentration of hydrolysis products during the first water vapor injection test	2-12
2-3.	Mean values and standard deviations of the concentrations of H ₂ , CO, and CO ₂ during stages in the first water vapor injection test	2-14
2-4.	The concentration of hydrolysis products during the second water vapor injection test	2-17
2-5.	The R/B value for ^{85m} Kr before, during, and after the first water vapor injection test	2-21
2-6.	Comparison of R/B for ^{85m} Kr values calculated by BFM and at Petten from measurements made during the first water vapor injection test	2-22
2-7.	The R/B values for ^{85m} Kr before, during, and after the second water vapor injection test	2-25

TABLES (Continued)

3-1.	The estimated values in each capsule of ^{85m}Kr R/B from contamination and from failed, designed-to-fail particles	3-4
3-2.	Calculation of the cumulative number of failed dtf particles at the times of R/B measurements in capsule A, B, and C	3-5
3-3. (a)	Failure times of the designed-to-fail (dtf) particles, fast fluences and fission rate densities for experiments HRB-17/18 and HFR-B1	3-8
3-3. (b)	Fast fluence and fission density at completion of designed-to-fail (dtf) particle failure in experiments HRB-17/18 and HFR-B1	3-8
4-1.	Transport times of downstream sweep gas for different decay volumes	4-3
4-2.	The ratio, R_f , of the (R/B)s correction factor for passage through a well-mixed volume to that for passage through a tubular segment of the same volume	4-9
5-1.	Calibration of gas chromatograph before, during, and after the water vapor injection test	5-2
5-2.	Data on the gas chromatogram area and concentration of the hydrolysis products H_2 , CO , and CO_2 before, during, and after the first water vapor injection test	5-3
5-3.	Data on the concentration of the hydrolysis products H_2 and CO measured gas chromatographically during the second water vapor injection test	5-9
6-1.	Incremental total count rates at a series of delays prior to gamma counting the fission gas sample taken from capsule C at 0049 on June 12, 1987	6-4
6-2.	Calculation of the count and delay time corrected number of accumulated counts for measurements on a sample taken from capsule C at 0049 on June 12, 1987	6-5
6-3.	Calculation of the count and delay time corrected number of accumulated counts for measurements on a sample taken from capsule C at 1410 on June 16, 1987	6-8
6-4.	The relative number of atoms of selected isotopes in the fission gas sample at the moment of collection	6-10

TABLES (Continued)

6-5.	Constants and parameters needed in calculation of the number of atoms of an isotope present in a fission gas sample	6-11
7-1.	Quantities needed to calculate the relative R/Bs for the fission gas sample taken from capsule C on June 15, at 1105 and measured as spectrum 2349	7-4
7-2.	The calculation of relative R/B values and comparison with reported values for the fission gas sample taken from capsule C on June 15 at 1105 and measured as spectrum 2349 Relative (R/B) values corrected to release from the fuel element and relative efficiencies	7-7
8-1.	Data taken from the raw gamma counting records (see Section 9) and calculation of the isotope specific quantity Q (See Eq. 8-2)	8-2

1. INTRODUCTION

This is an informal memorandum on various aspects of the HFR-B1 experiment. Ostensibly, this memorandum treats the first two water vapor injection tests in HFR-B1 conducted during my visit to Petten, but there are subsidiary issues which need to be addressed at the present. Some of the issues are related to my own lack of understanding and the questions which I raise are in the interest of better understanding, improving the experiment, and facilitating the analysis. In spite of the length of this memorandum, the analysis of what has already transpired is not nearly complete and is, moreover, mainly qualitative.

Comments and questions about this memorandum are solicited, particularly in response to Section 10 (below) which contains my own comments, questions, and requests. A Table of Contents, which is a needed guide to this memorandum, precedes this introduction. Please regard this memorandum not only as informal, but as a "working" memorandum, i.e., one that requires changes.

2. THE FIRST WATER VAPOR INJECTION TESTS IN HFR-B1

Two water vapor injection tests have been performed in capsule C of the HFR-B1 experiment during cycle 87.05. In examining and partially analyzing the results of these tests, I shall focus on four quantities: (1) the concentration of water vapor injected into the capsule; (2) the concentration of water vapor leaving the capsule; (3) the species and concentrations thereof resulting from the hydrolysis of carbonaceous and fuel material; and (4) the fission gas release before, during, and after the injection of water vapor. These quantities will be considered in order.

2.1. THE INJECTION AND DISCHARGE OF WATER VAPOR

The first water vapor injection tests continued for 6.2 h with a nominal water vapor concentration of 155 ppmv at 0.1 MPa between 1030 and 1644 on June 16th. Note that the hygrometer reading was nominally 50 ppmv, but that the pressure of the gas stream was about 0.31 MPa.

The second water vapor injection test continued for 95.1 h with a nominal water vapor concentration of 62 ppmv at 0.1 MPa between 1226 on June 20th to 1130 on June 24th. Note that the hydrometer reading was nominally 20 ppmv at a gas pressure of about 0.31 MPa.

The water vapor level in the outlet gas is presented in Table 2-1 for both tests. The magnitude of the water vapor concentration is given only in mV of recorder per displacement. The conversion from mV to ppmv or other concentration units will be made later. The times listed in Table 2-1 were arbitrarily selected from a continuous recording of the discharged water vapor.

TABLE 2-1

WATER VAPOR LEVEL IN THE OUTLET GAS FROM CAPSULE C BEFORE,
DURING, AND AFTER THE FIRST TWO WATER VAPOR INJECTION TESTS

Time(b)	Test No. 1		Test No. 2		
	Relative(c) Time (h)	Signal(d) (mV)	Time(b)	Relative(c) Time (h)	Signal(d) (mV)
16/1030	0.00	6.0	20/1220	0.00	5.8
16/1100	0.50	6.0	20/1300	0.67	5.8
16/1200	1.50	6.0	20/1400	1.67	5.8
16/1430	4.00	6.0	20/1500	2.67	5.8
16/1447	4.28	6.0	20/1700	4.67	5.8
16/1458	4.47	8.0	20/1930	7.17	5.8
16/1500	4.50	10.2	20/1942	7.37	5.8
16/1504	4.56	12.0	20/1958	7.63	8.0
16/1511	4.68	13.0	20/2004	7.73	9.0
16/1517	4.78	13.1	20/2007	7.78	9.2
16/1530	5.00	13.0	20/2107	8.78	10.4
16/1730	7.00	13.5	20/2507	12.78	10.4
16/1747	7.28	13.8	21/0300	14.67	10.2
16/1847	8.28	13.0	21/1500	26.67	10.2
16/1947	9.28	12.0	22/0300	38.67	10.3
16/2100	10.50	11.0	22/1500	50.66	10.3
17/1500	28.50	8.0	23/0300	62.67	10.2
18/1500	52.50	7.2	23/1500	74.67	10.2
19/1500	76.50	7.0	24/0300	86.67	10.2
19/1711	78.68	~6.5	24/1500	98.67	9.3
20/1500	100.50	5.9	25/0300	110.67	7.8
			25/1500	122.67	7.1
			26/0300	134.67	7.1

(a) These data are subject to revision upon more accurate measurement. At present, the water vapor level is given in terms of the voltage excursion (signal) of the recorder.

(b) The day and 24 h clock time are given as day/clock time. All data were taken in June 1987.

(c) The relative time is the time measured from the beginning of the water vapor injection; for test 1, the injection began at 16/1030 and for test 2, at 20/1220. The water vapor injection tests ended at 16/1644 for test 1 and at 24/1130 for test 2. Relative time = $24 \cdot (d - d_0) + (h - h_0)$ where d is day number, h the decimal hour, and symbols with subscript zero are the corresponding initial values.

(d) The signal values prior to the beginning of the water vapor injection tests were 6.0 and 5.8 for tests 1 and 2, respectively.

The water vapor level profiles are shown in Fig. 2-1 for the two water vapor injection tests. Before and immediately after the beginning of the injection of water vapor, the outlet gas from capsule C indicates no change in the signal. Thus, none of the water vapor added to the capsule is leaving it. After a definite time, depending on the water vapor concentration, water vapor suddenly appears in the outlet gas. The transition occurs within 1.5 h. Following this, the water vapor in the outlet gas remains at a constant level until the injection is terminated. Thereafter, the water vapor level in the outlet gas gradually decreases. Thus, there are three stages in the interaction of water vapor with the fuel elements in the capsule: (1) first, water vapor is consumed by reaction with and by sorption on components of the fuel element; (2) after a definite time, the reaction and sorption cease, or occur to a smaller extent - it is likely that in the sequence of processes involved in the reaction, of which this sorption process is likely to be one, the process becomes constrained and slows the overall consumption of water vapor; and (3) after the termination of water vapor injection, the sorbed water molecules are gradually desorbed and thus appear in the outlet gas to a declining extent. The sorption of the incoming water molecules with subsequent reaction of the sorbed molecules, eventual saturation of the sorption sites, and desorption following termination of water vapor injection is a suitable basis for understanding the profiles of Fig. 2-1. This basis is qualitatively examined as follows: [Note that thus far (and in what follows) the implicit assumption that hydrolysis of carbonaceous material, in comparison with fuel material, is predominately occurring. Detailed analysis is required to verify this assumption. Measurement of hydrolysis products is inadequate, since the same products occur in the hydrolysis of both carbonaceous and fuel material.]

Consider the time interval between the beginning of water vapor injection and of the appearance of water vapor in the outlet gas. The

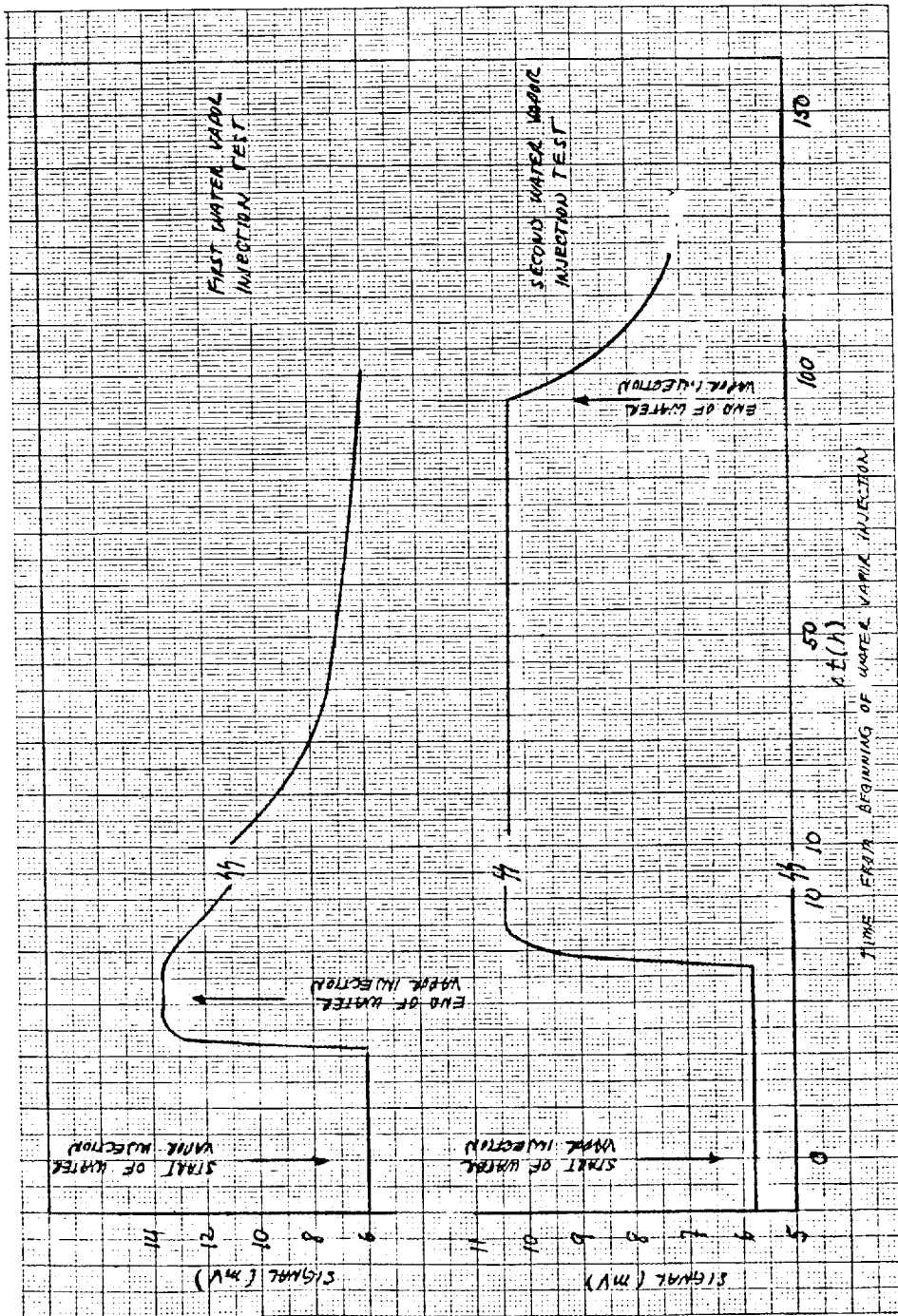


Fig. 2-1. The water vapor - time profiles in the gas outflow from capsule C

[MM-100-WORMM]

number of moles of water vapor added to the capsule within this time interval is given by

$$M_{H_2O} = \frac{CP}{RT} F_r t \quad , \quad (2-1)$$

where C = water vapor fractional concentration (ppmv/10⁶),

P = system pressure (MPa),

R = gas constant (= 8.314 MPa·cm³/mole·K),

T = temperature (K),

f_r = flow rate (cm³/min),

t = time (min)

at P = 0.31 MPa, T = 300 K, f_r = 300 cm³/min and C = 5 · E - 05 and 2 E - 05, and t = 257 and 442 min, respectively, in the first and second water vapor injection test, one finds correspondingly, 4.79 · 10⁻⁴ and 3.30 · 10⁻⁴ moles of water vapor added before the appearance of water vapor in the outlet gas. If the only process occurring were sorption, the water vapor would appear in the outlet gas after the same number of moles had been added to the capsule, since the number of sorption sites would be the same (ideally) in both tests. If, on the other hand, reaction were occurring after adsorption, then more sorbed water molecules would have reacted prior to saturation (or the appearance of water vapor in the outlet gas) in the test with the higher concentration of water molecules - which is what happened.

During the transition period between no changes in the water vapor signal in the outlet gas and the establishment of a constant higher signal, the balance between sorption and desorption following reaction is being established. That this transition requires about 1.5 h and not some time period of a different magnitude is related to the rate of desorption following reaction. A quantitative analysis should lead to an estimate of this rate, but is deferred for the time being.

During the period of the constant level of water vapor in the outlet gas, the balance between adsorption of water molecules and desorption of reaction products has been established. Thus, for a saturated surface, the desorption of reaction products is constant, the adsorption of water molecules is constant, and the remaining concentration of water molecules in the outlet gas is constant. Given the concentration of reaction products during this period, the desorption rates or reaction rates per site might be deduced. However, the ratio of the signals corresponding to water vapor in the outlet gas for the cases of inlet fractional concentrations of $5E-05$ and $2E-05$ is 1.7 not 2.5. $[(13.8 - 6) / (10.4 - 5.8) = 1.7$ from data of Table 2-1 and Fig. 2-1)]. If the number of adsorption and reaction sites were the same in both tests, then the ratio of the outlet gas water vapor concentrations would be expected to be closer to 2.5. The deduction that there is less water vapor in the outlet gas from the first test (with $C = 5 \cdot E - 05$) than expected in this case would indicate that there are other adsorption sites at which adsorption but not reaction is occurring. A good candidate for these sites would be the graphite on which hydrolysis is not expected to occur significantly at the low temperatures of the graphite in these tests. In fact, adsorption on the graphite could occur in both tests, but because of the higher water vapor concentration in the first test, more adsorption on graphite would occur and would deplete the gas phase of water molecules to a greater extent proportionately in the first test; hence, a ratio of concentrations in the first to second test less than 2.5 could be expected.

It must be appreciated at this point that sorption on sites with subsequent reaction will destroy the original sites and that the implicit assumption in the discussion above has been that the newly created sites are of the same structure, in general, as the previous sites. The fact that a saturation level appears to be reached indicates that the number of accessible sites, original and derived, is limited and is approximately constant in time.

A consequence of the discussion above is greater adsorption of water vapor on the carbonaceous material in the first rather than the second water vapor injection tests. This being so, a greater amount of water vapor should appear in the outlet gas in the first test after termination of water vapor injection. This is the case as shown in Fig. 2-2 where the profiles of signals corresponding to the water vapor concentration are shown. The areas under the curves are proportional to the amount of water molecules desorbed from the fuel element surfaces, and the ratio of the areas for the first to the second test is about 1.3. The rationalization for expecting a larger quantity of desorbed water molecules from the test with an injected fractional concentration of $5E-05$ than from that with a value of $2E-05$ has been stated above. However, this matter is not as straight forward as I have presented it. The total quantity of water vapor injected in the second test was six times that injected in the first. Thus, the observation of greater sorption in the first test can only be understood if a steady-state distribution between the gas and surface phases was established during water vapor flow through the capsule. In this case, there would be a limited surface area accessible on which sorption occurred. This surface area would consist as deduced above of reactive and nonreactive ^{sites} surfaces. The former would reach a state in which all sites were occupied by sorbed water molecules or dissociation products, thereof; whereas, the latter would have sorbed a quantity of water molecules proportional to the water vapor pressure (and not to the accumulated exposure to water molecules). In this way, the larger quantity of desorbed water molecules in the outlet gas from the first test can be understood in spite of the much greater exposure of the surfaces in the second test to water vapor. Yet this is not all. One might argue that the extent and structure of the sorption (including reactive sites) might have been altered following the first test so that the above explanation is either incorrect or incomplete. This possibility is open to testing by simply attempting to repeat the first test.

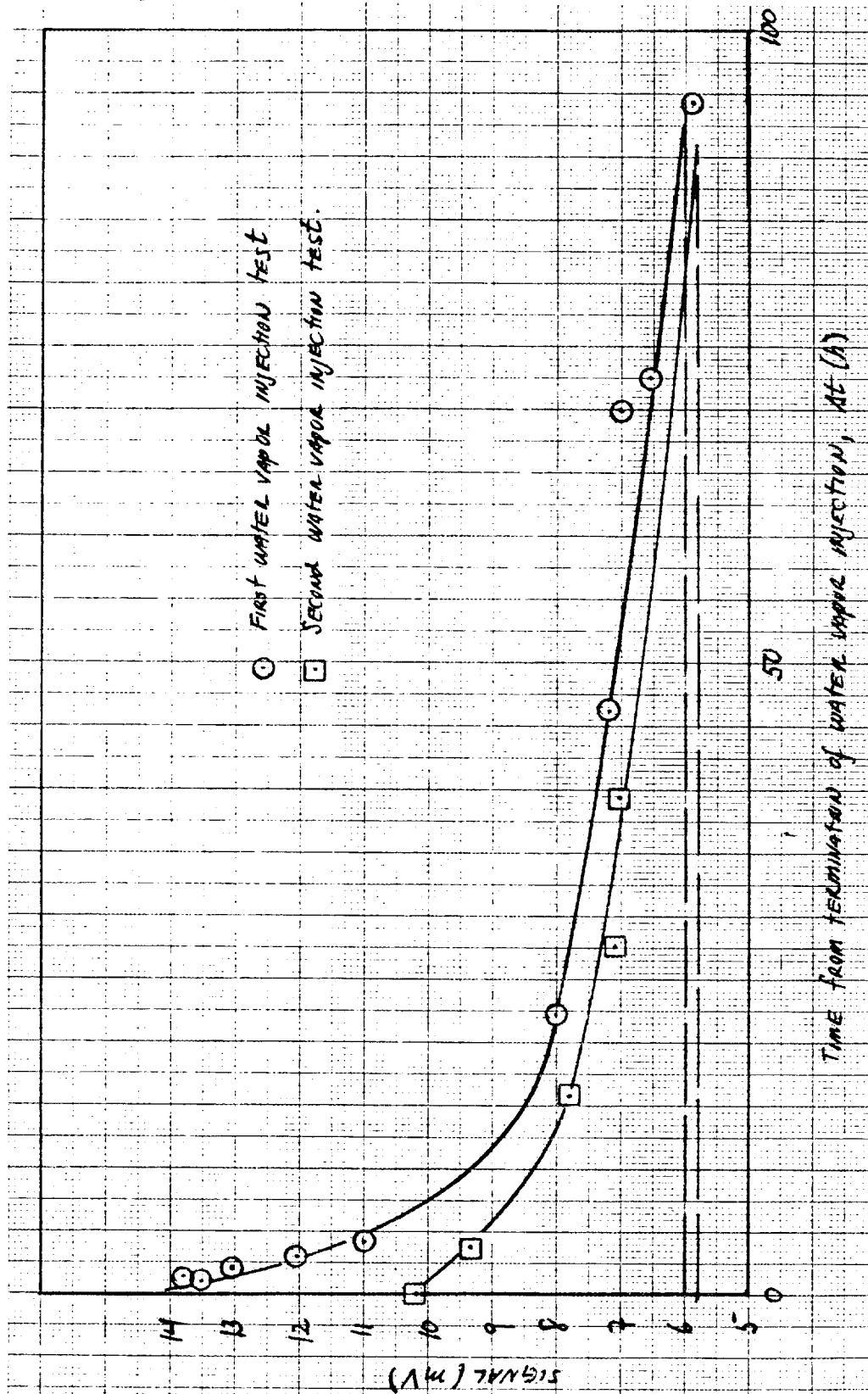


Fig. 2-2. Time profiles of water vapor in outlet gas from capsule C following termination of water vapor injection

The discussion thus far has been qualitative; or, at best, semi-quantitative and, furthermore, contains speculative elements. Thus, it represents only a beginning of the analysis.

The conversion from the hygrometer signal in mV to the water vapor concentration requires a conversion factor that can be supplied from the experiments. Alternatively, and in the meantime, an estimate of the conversion factor can be made from measurements of the reaction products of hydrolysis as reported below. Thus, I shall return below to the topic of water vapor outlet concentrations.

2.2. THE HYDROLYSIS OF CARBONACEOUS MATERIAL

The reaction of water vapor with the carbonaceous materials in the fuel elements is one of the two major phenomena to be studied in capsule C of HFR-B1. The primary result of the hydrolysis is embodied in the reaction



Thus, the reaction products are primarily hydrogen and carbon monoxide. Of importance in the analysis is the equality of the molar quantities of water, hydrogen and carbon monoxide as a result of this reaction. In Eq. 2-2, $\text{C}_{(s)}$ represents the carbonaceous material as a solid (s). Clearly, as the reaction proceeds, the $\text{C}_{(s)}$ is removed and appears as carbon monoxide; and so, the surface on which reaction occurs is continually changing. In actuality, for the first and second water vapor injection tests, not only were hydrogen and carbon monoxide, but also carbon dioxide detected; no methane has thus far been detected. The amount of carbon dioxide detected is a small fraction of the carbon monoxide. The reaction by which carbon dioxide is produced is less certain

than the overall process given above for carbon monoxide production, but one might consider the overall process,



as a candidate. Note again that thus far, and in what follows, the implicit assumption that hydrolysis of carbonaceous material in comparison with fuel material is predominately occurring. Detailed analysis is required to verify this assumption.

In studying the hydrolysis of carbonaceous material, one must be careful to exclude oxygen from the capsule as the oxidation (by O_2) of the carbonaceous material is much more rapid than the hydrolysis. Thus, a small quantity of oxygen relative to water vapor could significantly distort an analysis based on a hydrolysis reaction. Bearing on this matter was the observation following the first water vapor injection test of a relatively high $\text{O}_2 + \text{N}_2$ content of the gas sample from chromatographic analysis. A series of tests was begun to detect oxygen upstream of the capsule. It was determined that the $\text{O}_2 + \text{N}_2$ did not originate upstream of the capsule by gas chromatographic measurements of the gas stream when (a) the water vapor generating system was bypassed but the capsule was in the flow system, (b) the capsule was bypassed using gas from the helium and neon supply system, and (c) the capsule was bypassed and the water generating system with and without the GEI hygrometer was in the system.

The products of the reactions given above (see Eqs. 2-2 and 2-3) were measured gas chromatographically. A more detailed discussion of the measurements and problems associated with the measurements is given in Section 5. For present purposes, only two problems need be recognized: (1) during the second water vapor injection test, a neon contamination seriously interfered with the measurement of hydrogen and (2) the automatic integration of the areas under the peaks of the chromatogram can be highly unreliable. The first problem can be best solved

by excluding the neon contamination. The second problem is, at this time, a mystery to me and probably requires a detailed knowledge of the operation of the gas chromatograph. More information on both problems is given in Section 5.

The results of the GC measurements of H₂, CO, and CO₂ before, during, and after the first water vapor injection test are presented in Table 2-2 and plotted in Fig. 2-3. Also shown in Fig. 2-3 is the profile for the water vapor content of the effluent from capsule C (these data have been presented above in Table 2-1 and Fig. 2-1). The horizontal lines on the upper half of Fig. 2-3 represent the mean values, over the time interval indicated, of the reaction products H₂, CO, and CO₂. The important general results embodied in Fig. 2-3 are:

1. During the first 4.4 h following the beginning of water vapor injection, the averaged value of the concentrations of H₂ and CO are the same within the uncertainties of measurement; the concentration of CO₂ is small compared to the concentrations of H₂ and CO.
2. When water vapor begins to appear in the effluent from capsule C, the average concentrations of H₂ and CO are substantially reduced (by factors between 3 and 30); the concentration of CO₂ increases by 50%.
3. After termination of water vapor injection, the concentrations of H₂, CO, and CO₂ return to nearly the prehydrolysis values.

The mean values and standard deviations of the concentrations of H₂, CO, and CO₂ are presented in Table 2-3. The mean values are represented by horizontal lines in Fig. 2-3. Corrected for background, the mean concentrations of H₂, CO, and CO₂ become 198, 227, and 16 ppmv at 0.1 MPa during stage 2 (see Table 2-3 for definition of stages) with corresponding standard deviations of 72, 55, and 12, respectively.

TABLE 2-2

THE CONCENTRATION OF HYDROLYSIS PRODUCTS
DURING THE FIRST WATER VAPOR INJECTION TEST

Date	Time	Relative Time (h)	Concentration (ppmv at 0.1 MPa)		
			H ₂	CO	CO ₂
June 16	0955	-0.58	0	10	0.2
	1004	-0.52	47	7	4.0
	1034	0.067			12
	1045	0.25	134		15
	1102	0.53	279	309	25
	1111	0.68			4
	1128	0.97	231	208	
	1139	1.15			
	1150	1.33	135		10
	1200	1.50		241	
	1212	1.70	181	166	11
	1246	2.27	291	178	43
	1306	2.60	281	243	
	1425	3.92	296	295	
	1433	4.05	172		23
	1459	4.48	40	7	28
	1509	4.65	113	7	37
	1519	4.82	43	97	31
	1527	4.95	43	304	31
	1527	4.95	86	489	32
	1546	5.27	42	8	26
	1603	5.55	125	237	26
	1630	6.00	64	187	48
2029	9.98	26	0	0	
2048	10.30	24	0	0	
2103	10.55	25	0	0	

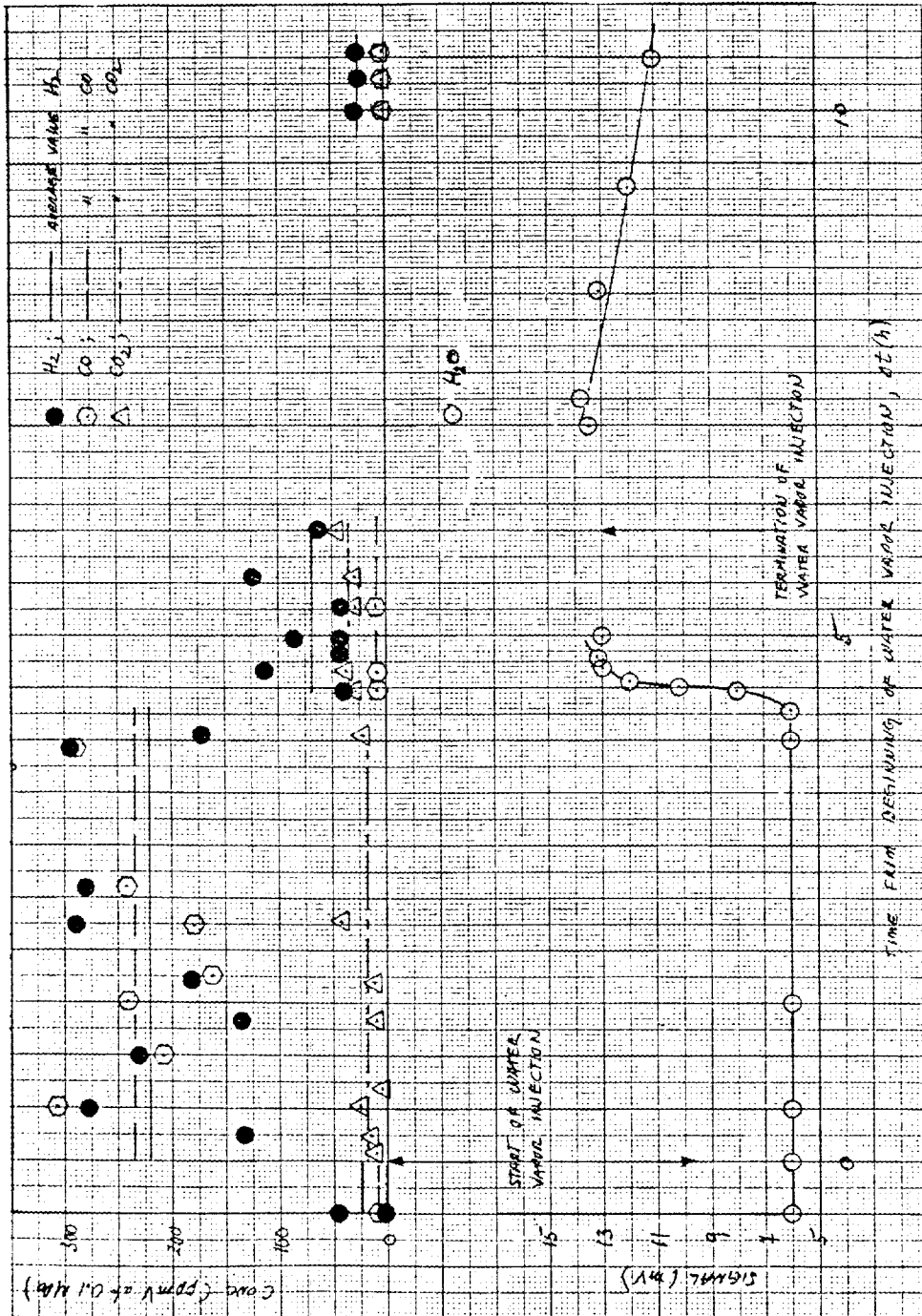


Fig. 2-3. Time profiles of H₂, CO, CO₂, and water vapor in capsule C

TABLE 2-3
 MEAN VALUES AND STANDARD DEVIATIONS OF THE CONCENTRATIONS OF
 H₂, CO and CO₂ DURING STAGES IN THE FIRST WATER VAPOR INJECTION TEST

Stage	Stage Definition	H ₂	CO	CO ₂
1	Prehydrolysis, Δt (h) < 0	23.5 ± 23.5	8.5 ± 2.1	2.1 ± 2.1
2	Hydrolysis - 1, $0 \leq \Delta t$ (h) \leq 4.4	222. ± 68.	234. ± 55.	17.9 ± 12.2
3	Hydrolysis - 2, $4.4 < \Delta t$ (h) \leq 0.2	69.5 ± 34.4	7.3 ^(a)	27.4 ± 8.6
4	Posthydrolysis $9.9 \leq \Delta t$ (h) \leq 10.6	25. ± 1.	0.0	0.0

(a) The abnormally high values for CO between 4.48 and 6.00 h after the start of water injection are attributed to the unreliability of the automatic integration of peaks by the GC system. (See text and Section 5.)

The concentration of water vapor injected was 155 ppmv at 0.1 MPa. Consequently, within the uncertainties of the concentrations and according to Eq. 2-1, (the following conclusions are made):

1. The molar quantities of the reaction products H_2 and CO are the same.
2. The molar quantities of the reactant H_2O and the product H_2 are the same.
3. The molar quantities of the reactant H_2O and the product CO differ by more than the known uncertainties.
4. The sum of the molar quantities of CO and CO_2 and of H_2 are the same.

The general conclusion is that hydrolysis is occurring in accordance with the reactions given as Eqs. 2-2 and 2-3 above. If, however, one's faith is placed in the average values of the concentrations, then other possibilities arise. In particular (the following results are possible):

1. The measured concentration of the water vapor added could be lower than the actual value by 20 to 30%.
2. The unreliability of the integration processing of the GC could result in average values of H_2 and CO that would be too high.

The concurrent hydrolysis of exposed fuel, which as shown below is occurring, would not affect the discrepancies among the mean concentrations of H_2 , CO and CO_2 .

The results of the GC measurements of H₂ and CO during the second water vapor injection test are presented in Table 2-4 and in Fig. 2-4. The data are meager for reasons discussed in Section 5. The hydrogen measurements at 24.3 h after the start of the water injection consist of two groups: in one, the concentration is 68 ppmv with a very small standard deviation; and in the other, it is 2.4 times larger. Since the concentration of added water vapor was 62 ppmv, the higher values are clearly in error. The lower valued group has a concentration just about equal to that of the added water vapor and thus, in this case, the H₂/H₂O ratio is one as expected for hydrolysis of carbonaceous material. The low values of CO are not explicable, except perhaps in terms of the hardly detectable CO peaks in the chromatograms. Thus, for practical purposes, the use of water vapor concentrations less than (or even comparable) to 60 ppmv at 0.1 MPa introduces some difficulties in GC detection of species.

2.3. THE HYDROLYSIS OF THE FUEL UCO

The reaction of water vapor with the fuel, UCO, is the second of the two major phenomena to be studied in capsule C. As a result of the hydrolysis of the fuel, two general processes occur: the hydrolysis of the fuel, embodied in the two reactions



and



as well as increased steady-state release of fission gas

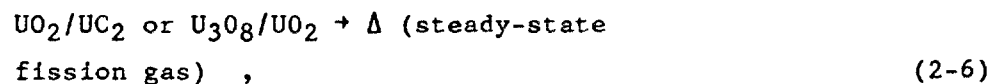


TABLE 2-4

THE CONCENTRATION OF HYDROLYSIS PRODUCTS DURING
THE SECOND WATER VAPOR INJECTION TEST

Date	Time	Relative Time (h)	Concentration (ppmv at 0.1 MPa)	
			H ₂	CO
June 21	1245	24.3	68	
			68	
			156	
			165	
			67	~33
June 22	1600	51.6	≥28	19
June 24	1130	95.1	---	3.9
June 25	1015	117.8	---	

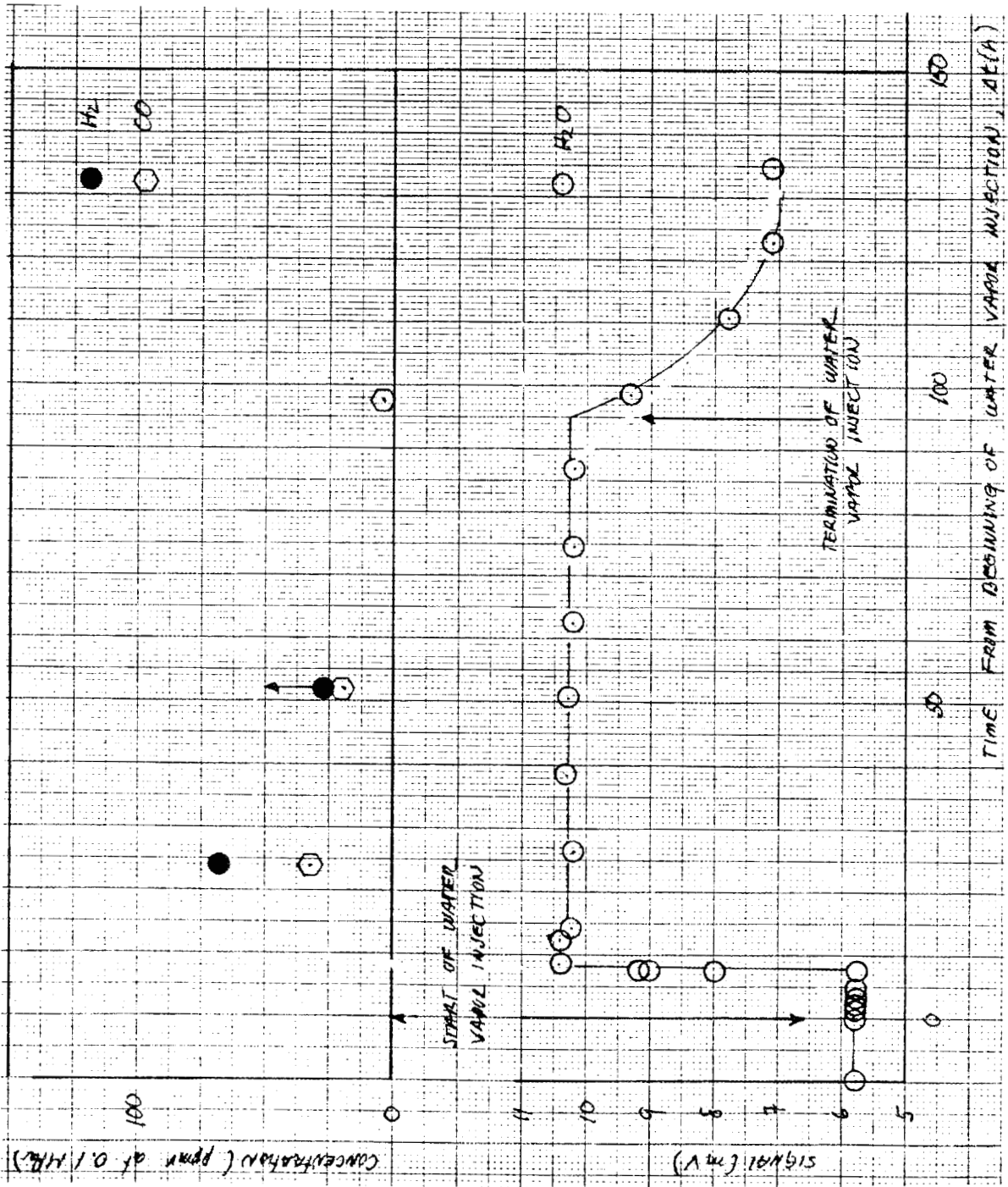
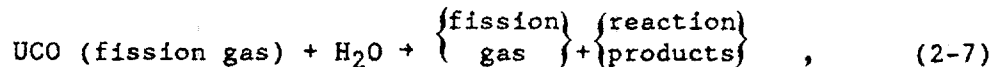


Fig. 2-4. Concentrations of H₂ and CO and time profile of water vapor in capsule C effluent for the second water vapor injection test

i.e., the hydrolysis of the fuel has the two major results: (1) change in the chemical and structural state of the fuel and (2) increased release of fission gas of the altered fuel. The latter result may or may not persist for longer periods of time depending on the state of the altered fuel. There are also two other results of lesser importance for capsule C. The first result is as follows:



where the fission gas refers to that portion of the fission gas stored within the fuel; i.e., gas that cannot escape from the fuel readily because the gas atoms are interstitially held or are retained in grain boundary pores. The following is the second result:



where M represents a metallic fission product atom not yet bound as an oxide.

Note that in the major reactions, (Eq. 2-4 and Eq. 2-5), the molar quantities of H₂ and CO (in one case) and the molar quantity of H₂ (in the other) are the same as the molar quantities of H₂O. However, in principal, reaction 2-5 (Eq. 2-5) can be distinguished from reaction 2-4 (Eq. 2-4) via the H₂/CO ratio. The main evidence that hydrolysis of the fuel occurred in the first two water vapor injection tests is the detection of increased steady-state fission gas release; i.e., Eq. 2-6. Following the injection of water vapor, the detection of H₂ and CO indicates that fuel hydrolysis as well as hydrolysis of carbonaceous material can be occurring. The relative contributions of the hydrolysis of fuel and carbonaceous material to the production of H₂ and CO remains to be determined.

Before presenting the fission gas release measurements for either of the two water vapor injection tests, I will address two problems -

one of which may result from my lack of knowledge of the ingredients in the calculation of R/B at Petten. The first problem involves the time associated with the R/B measurements reported (HFR/87/2380). By comparing the various times listed on the raw data sheets I received while at Petten with the reported times, it is clear that the reported times represent the start of counting and not the times at which the gas sample left the reactor. The use of counting times in the analysis would introduce a distortion. A better reporting procedure would be to use the time of collection of the sample which is listed on the raw data sheets with an indication as to whether a correction has been made to account for the decay of the radioactive isotopes between collection and the start of counting or has not been made. In any case, a future correction for decay between release of the gas from the fuel and collection of the gas sample, although not relatively large for the isotopes normally being measured, would have to be made. In treating the R/B data from the first water vapor injection test, I have used the collection times reported on the raw data sheets in my possession (although I do not know to what times the R/Bs have been back corrected for decay). In treating the R/B data from the second water vapor injection test, the reported times have had to be used but errors in times associated with these data make comparison with reaction product - or water vapor discharge - profiles uncertain.

The second problem involves my attempt to calculate relative values of the R/B for ^{85m}Kr from the raw data for the first water vapor injection test (see Section 8). The method by which I calculated the relative R/Bs is given in Section 8 based on considerations in Sections 6 and 7. The R/B data for ^{85m}Kr reported by Petten are presented in Table 2-5 and the comparison of these with my calculation is presented in Table 2-6. (Note that I have retained the total fissile loading as the basis of the ^{birth}~~bulk~~ rate.) All data are presented in Fig. 2-5 along with the water vapor discharge profiles.

TABLE 2-5
 THE R/B VALUE FOR $^{85}\text{m Kr}$ BEFORE, DURING, AND AFTER
 THE FIRST WATER VAPOR INJECTION TEST

Date	Collection Time	Spectrum No.	Relative Time (h)	R/B for $^{85}\text{m Kr}$
June 15	1105	2349	-23.4	6.51 E-04
June 16	0842	2362	-1.8	6.85 E-04
June 16	1418	2366	3.8	9.24 E-04
June 16	2100	2369	10.5	9.43 E-04
June 17	1710	2379	30.7	6.62 E-04
June 18	1300	2389	50.5	1.05 E-03
June 19	1100	2399	72.5	9.36 E-04
June 20	0936	2409	95.1	5.08 E-04

TABLE 2-6
 COMPARISON OF R/B FOR $85^m K_r$ VALUES CALCULATED BY BFM AND AT PETTEN
 FROM MEASUREMENTS MADE DURING THE FIRST WATER VAPOR INJECTION TEST

Relative Time (h)	Q(a)	R/B Calculated	R/B Reported
-23.4	1.20 E+07	6.68 E-04(b)	6.51 E-04
-1.8	1.18 E+07	6.57 E-04	6.85 E-04
3.8	1.21 E+07	6.74 E-04	9.24 E-04
10.5	1.36 E+07	7.57 E-04	9.43 E-04
30.7	1.34 E+07	7.46 E-04	6.62 E-04
50.5	1.28 E+07	7.13 E-04	1.05 E-03
72.5	1.20 E+07	6.68 E-04	9.36 E-04
95.1	1.17 E+07	6.51 E-04	5.08 E-04

(a) See Section 8.

(b) Based on average R/B at -23.4 and -1.8 h before start of water vapor injection as reported by Petten.

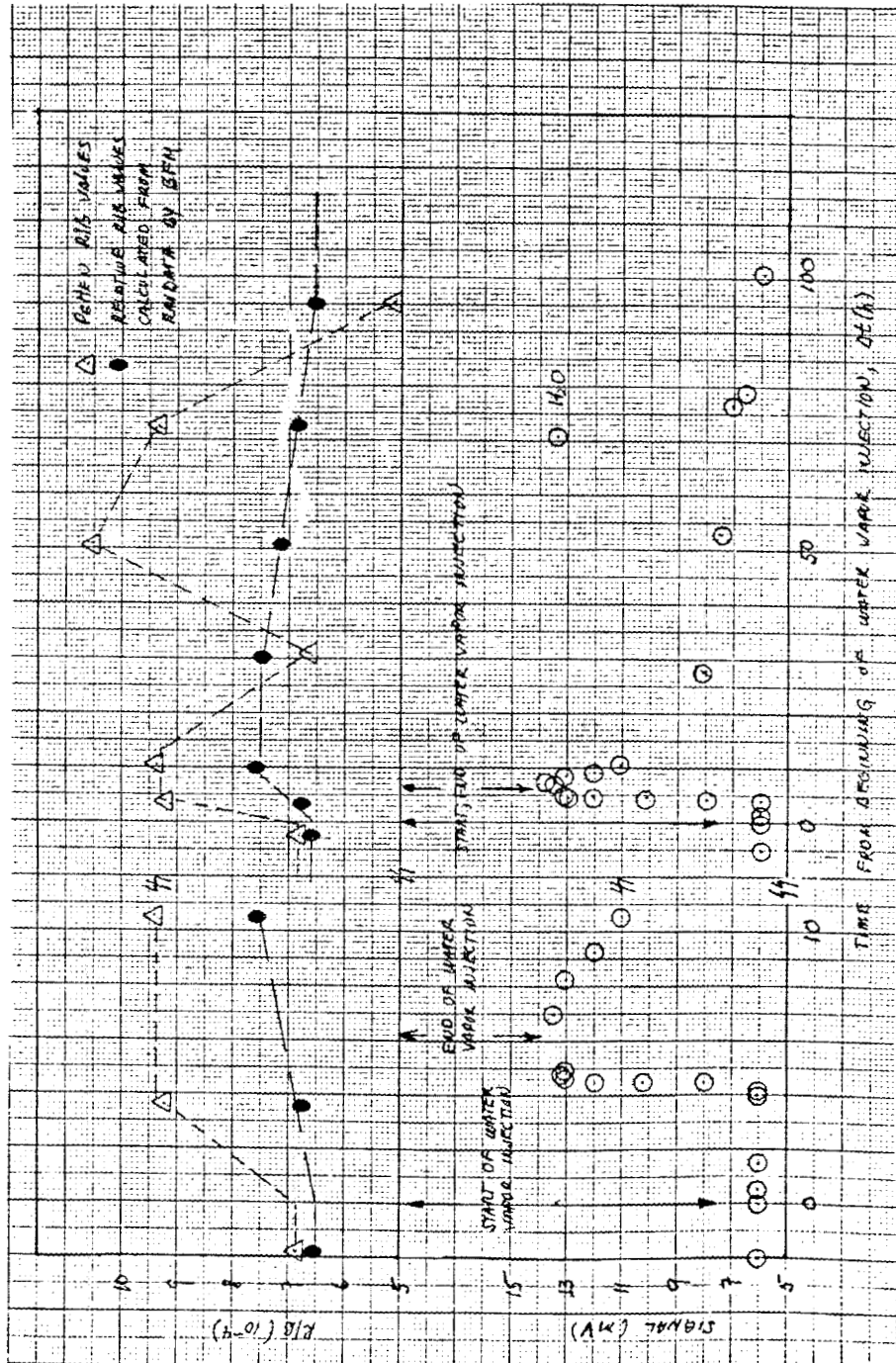


Fig. 2-5. Time profiles of R/B for ^{85m}Kr and water vapor discharge for the first water vapor injection test

The data of Fig. 2-5 clearly show that the addition of water vapor to the capsule results in an increase in the steady-state fission gas release. The R/Bs reported, as can be seen on the condensed time scale plot (on the right side), yield a profile inexplicable in terms of this test and in relation to what has been observed several times in the HRB-17/18 hydrolysis tests. There is no reason after the initial decline in R/B for a subsequent rise and fall in the profile. If this aberration were attributed to uncertainty in the measurements, then a quantitative analysis would become rather difficult. Furthermore, the reported R/B values leave the start of fuel hydrolysis in doubt. By contrast, the relative R/B values (normalized to the reported R/B value at -1.8 h) show a profile of reasonable shape and one in accord with the HRB-17/18 measurements. This, of course, does not validate the calculations of the relative R/B values; these calculations must be independently assessed. The relative R/B based profile indicates (1) a rise in the R/B beginning with the addition of water vapor (2) a continuation in the increase in R/B after termination of water vapor injection; this might be expected on the basis of diffusion of the water vapor into the regions of the kernel containing UC₂ (see below), (3) a period of constant R/B following termination of fuel hydrolysis and (4) a period of sintering or annealing of the hydrolyzed fuel resulting in a decrease in R/B to the initial value. This sequence is the same as that observed in HRB-17/18 for the UC₂ portion of the UCO fuel. On the other hand, the magnitude of the change in R/B just after the addition of water vapor for the Petten R/B values is in accord with that observed in the HRB-17/18 experiments; whereas, the corresponding R/B change based on the calculated relative R/B values is not.

In view of the uncertainties about the R/B values and the large variations in the reported R/B values, further analysis to determine the extent of fuel hydrolysis is not appropriate at this time.

The R/B values for the second water vapor injection test are presented in Table 2-7. Note that the relative times are based on the

TABLE 2-7

THE R/B VALUES FOR ^{85m}Kr BEFORE, DURING, AND
AFTER THE SECOND WATER VAPOR INJECTION TEST

Date	Counting Time	Relative ^(a) Time (h)	R/B for ^{85m}Kr
June 20	1130	-0.93	5.08 E-04
	1530	3.07	5.18 E-04
	1853	6.45	6.93 E-04
	2136	9.17	7.48 E-04
June 21	0252	14.4	7.22 E-04
	0542	17.3	7.89 E-04
	1106	22.7	9.48 E-04
	2057	32.5	1.11 E-03
June 22	0248 ^(b)	38.4	8.10 E-04
	0542	41.3	7.63 E-04
	1041	46.3	8.61 E-04
	1421	49.9	9.71 E-04
June 23	1033	70.1	8.33 E-04
June 24	1044	117.8	6.79 E-04
June 25	1017	94.3	8.02 E-04
June 26	1024	142.0	7.48 E-04
June 27	1148	167.	7.37 E-04
June 28	1106	191.	7.68 E-04

^(a)Calculated from starting time of June 20 1226 but relative values have an unknown error for being based on the time at the beginning of counting.

^(b)The value listed as taken on June 21 but this obviously is a typographic error.

time at which counting began; and, therefore, since the time at which the gas sample left the fuel must be used as a basis in order to compare the R/B values with other measurements such as the water vapor discharge time profile, the time scale of the R/B profiles is uncertain by times between about 2 and 6 h. The R/B time profile is presented in Fig. 2-6 along with the time profile of water vapor discharge. Again, the R/B clearly rises in response to the injection of water vapor; but following that, there are rather large excursions in R/B values and after the termination of water vapor injection, the R/B values remain at the level to which they initially rose. These results are not in accordance with HRB-17/18 observations. The magnitude of the changes in R/B are somewhat large for a concentration of 62 ppmv at 0.1 MPa. Given the initial rise in R/B values and the passage of time involved, the excursions (outlined by the dashed curves of Fig. 2-6) are unexpected. In the HRB-17/18 experiments (at 100 ppmv), excursions due to release of storage gas occurred with 5 h of water vapor injection and the largest excursion by far occurred within 1.5 h. In the present case, the excursions did not begin until after 14 h. However, to be considered in this regard is the shift in the R/B profile of Fig. 2-6 to earlier times when account is taken of the time the gas was released from the fuel rather than using as a reference time the start of counting. If the resulting shift were such as to bring into correspondence the rise in water vapor discharge and the beginning of the excursions (and the shifts are of the proper order), then the excursion might be attributed to a relatively high concentration level of water vapor invading the fuel kernel. Prior to the rise in water vapor discharge, the reaction of water vapor with the carbonaceous material would have reduced the amount of water vapor reaching the fuel. Nevertheless, one would still expect excursions, if detectable, to be observed during the initial rise since the initial rise has the same magnitude as the subsequent excursions. Another possibility results from taking into account the shift (as discussed above) and regarding the R/B values of $\sim 5 \cdot E - 4$ as aberrations. Thus, consider the base value of R/B to be $\sim 7.5 E - 04$. Then, there is no rise in R/B until the water vapor discharge rises and water

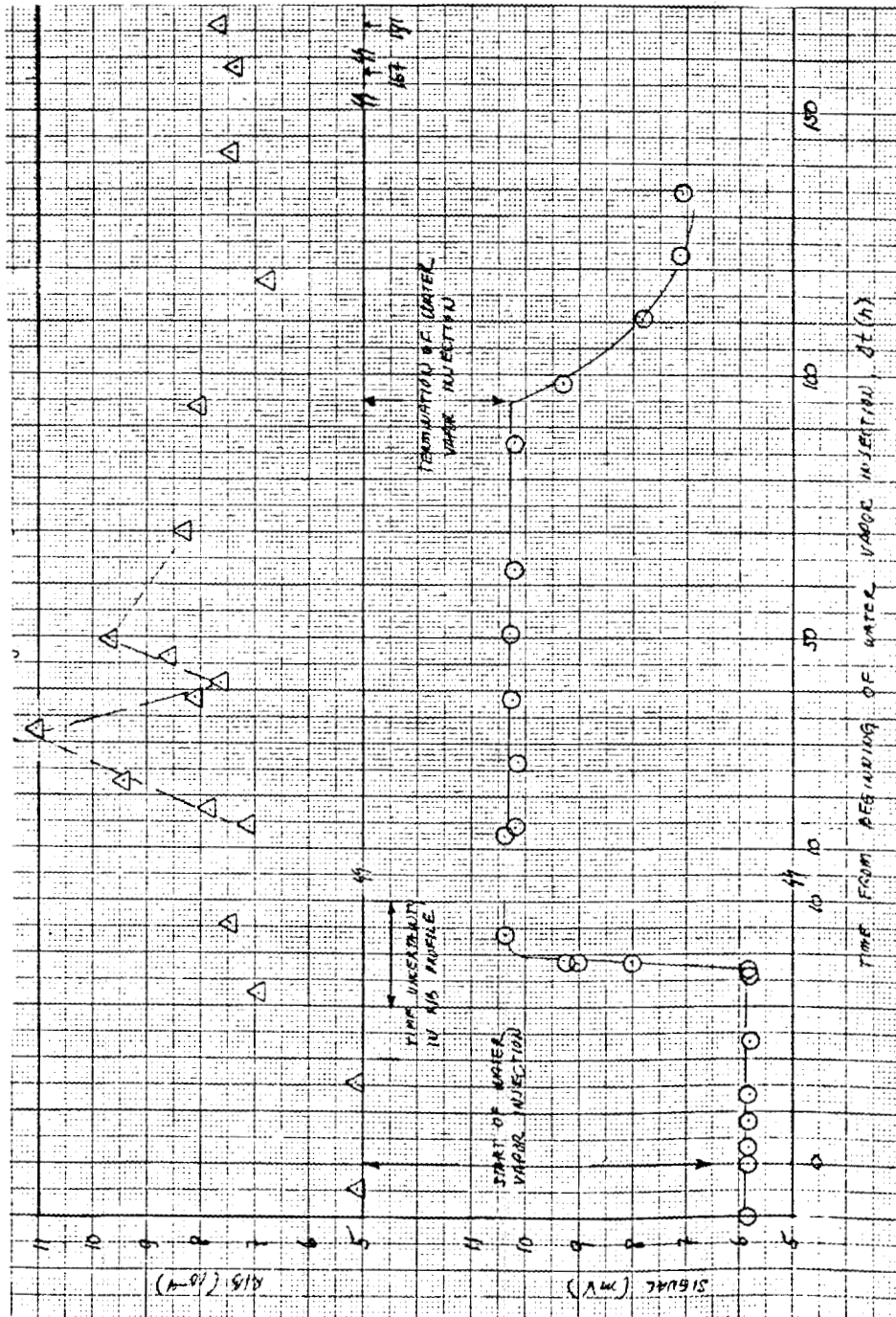


Fig. 2-6. Time profiles of R/B for 85m Kr and water vapor discharge for the second water vapor injection test

vapor becomes available to diffuse past the carbonaceous material and reach the fuel. The results of the first encounter of water vapor with the fuel is to release stored gas, but not to significantly hydrolysis the fuel. Consequently, after termination of water vapor injection, the R/B returns to its initial value. The extent of hydrolysis would be such as to release, on the average, about $3E-03$ of the inventory of stored gas from each particle (recall that only 8.76% of the fissile particles are dtf particles and to make any absolute calculation, one must correct the R/B values to a basis of dtf particles.) Consequently, the extent would be equivalent to hydrolyzing a surface layer of the spherical kernel 200 nm in thickness. The amount of water vapor required to accomplish this extent of hydrolysis is rather small and would not present a problem.

The above possibilities for understanding the R/B profile for the second water vapor injection test are speculative. Before going further, the questions raised concerning the R/B values of the first water vapor injection test need to be resolved, at least from the analyst's viewpoint.

2.4. THE SOURCE OF THE H₂ AND CO

As mentioned above, H₂ and CO can be produced as a result of the hydrolysis of fuel as well as of carbonaceous material. The relative production rates are of primary interest. What is the evidence that predominately carbonaceous material is being hydrolyzed?

At this stage in the development of the Petten experiments, the best evidence comes from comparing the present experiment with the results of the hydrolysis experiment in HRB-17/18. In the latter experiment, 100 ppmv of H₂O at a pressure of about 0.1 MPa and at a flow rate of about 120 cm³/min passed over 6 fuel compacts of the same design containing a total of 30 failed dtf particles for a period of 12 days. At a temperature of 300 K (assumed measurement temperature of the water

vapor concentration), the H₂O fluence (see Eq. 2-1) was 8.4.E-03 mol. The UC₂ fuel in the UCO dtf particles was hydrolyzed to the extent of not more than 14% as determined by comparing the incremental increases in R/B in this case with that observed after complete hydrolysis of the UC₂ portion. As the 30 dtf particles required only 1.1 E-05 mol H₂O to have all the UC₂ hydrolyzed, only 2.E-04 of the H₂O passing by the fuel rods actually participated in a hydrolysis reaction involving UC₂. The corresponding experiment in Petten involved 155 ppmv at 0.1 MPa at a flow rate of 300 cm³/min passing over 12 fuel compacts containing 1044 failed dtf particles for a period of 4.5 h. The H₂O fluence in this case was $4.8 \cdot 10^{-4}$ mol, a factor of 18 smaller than in the HRB-17 experiment cited. The 1044 failed dtf particles require $3.7 \cdot 10^{-4}$ mol H₂O for complete hydrolysis. If the fraction of the H₂O fluence participating in hydrolysis was 1.55 times as large as the HRB-17 case (i.e., accounting for the dependence of the rate of hydrolysis on water vapor pressure), then the extent of reaction in the present case was only 0.04%.

This explanation of the predominance of the hydrolysis of carbonaceous material concentrates on the hydrolysis of the UC₂ portion of the UCO kernel, because the results of the HRB-17 experiment clearly show that the carbide portion is hydrolyzed before the UO₂ portion; and, therefore, in the very short time - first water vapor injection test of Petten only the carbide is participating in the hydrolysis. (Note that in calculating the amount of H₂O required to hydrolyzed the UC₂ portion of the UCO kernel, Eq. 2-4 and the following data on UCO kernel were used; 347 μm kernel diameter, 10.51 Mg/m³, and 0.2 fractional UC₂ content.)

Another argument for the predominance of the hydrolysis of carbonaceous material resides in the water vapor discharge profiles. The hydrolysis of carbonaceous material is, in one sense, a repetitive process; i.e., the carbon atoms on reactive sites are consumed by reaction

[MM-100-WORMM]

but other carbon atoms replace them as reactive sites. By contrast, the hydrolysis of the carbon portion of the fuel occurs but once. Hence, the repetitive pattern in the water discharge profiles is unlikely to represent the hydrolysis of UC_2 . Again, this argument is based on understanding gained in the HRB-17/18 experiments and, in addition, is general.

3. THE FAILURE OF THE DESIGNED-TO-FAIL PARTICLES

The designed-to-fail particles (dtf), composing 8.76% of the fissile particles in the fuel elements of the experiments, were expected to fail early in the first Petten cycle (87.03). The fission gas release is the only measure of the failure available from measurements at the Petten reactor. These are shown for all three capsules (A, B, and C) in Fig. 3-1 where the R/B values are plotted against day number for the first cycle. The values of R/B shown in Fig. 3-1 are based on the birth rate of ^{85m}Kr in all fissile fuel containing particles. To obtain the R/B values based on only the fissile fuel in the dtf particles would require multiplying the R/B values, minus the contribution to R/B from heavy metal contamination, by $(0.0876)^{-1}$. This will be done below, but immediately, the basis of total fissile inventory will be retained.

From the data of Fig. 3-1, the time profile of the cumulative number of particle failed can be derived. Capsules A, B, and C will be considered separately. For the moment, the assumption will be made that by the end of the cycle, all dtf particles will have failed. This assumption will be justified below by considering the absolute value of R/B for a failed particle based on a comparison with the R/B of a just failed dtf particle as observed in HRB-17/18 where, in the latter case, no uncertainty as to the failure exists.

The R/B, at any time in the course of the process of dtf particle failure, is given by

$$(R/B) = (R/B)_c + \frac{N_f}{N_{dtf}} (R/B)_f \quad , \quad (3-1)$$

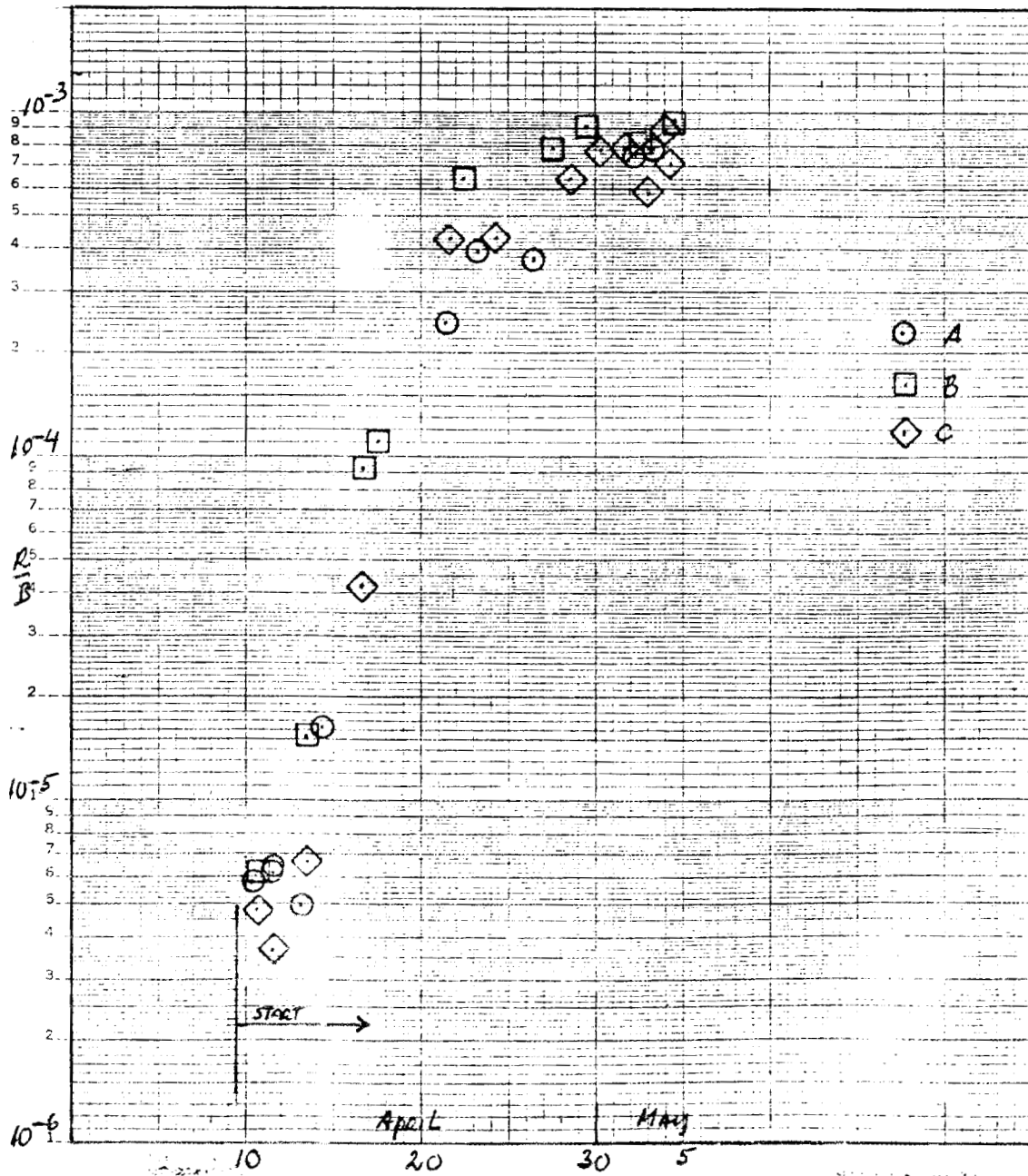


Fig. 3-1. Time profiles of R/B values for capsule A, B, and C during the period when the designed-to-fail particles were failing: cycle 87.03 (R/B values are based on total fissile loading)

where $(R/B)_c$ = contribution from contamination,
 $(R/B)_f$ = contribution from failed dtf particle,
 N_f = number of failed particles,
 N_{dtf} = number of dtf particles.

The values of $(R/B)_c$ and $(R/B)_f$ were determined by averaging a selected number of R/B values (from those shown in Fig. 3-1) at the beginning and at the end of the cycle. The deduced values of $(R/B)_c$ and $(R/B)_f$ and the number of data used in this process are shown in Table 3-1. Equation 3-1 was then used in conjunction with the data of Table 3-1 to determine the values of N_f corresponding to each R/B measurement time. The results are shown in Table 3-2 and plotted in Fig. 3-2. Least square straight line fits to the data of Table 3-2 are shown in Fig. 3-2; the coefficients of these fits are also given in Table 3-2. The data used in obtaining the least square fits include all data shown in Table 3-2 up to the time at which the calculated value of N_f first surpassed the value of N_{dtf} (= 1044).

The use of a straight line to fit the data of Table 3-2 and Fig. 3-2 is justified by the profiles of dtf particle failure observed in HRB-17/18. In the latter experiment, the failure of each particle was detected as a spike of gas release so that no uncertainty existed as to the moment of failure of each particle and also as to the number of particles failed (the latter number was identical to the number of dtf particles present). The cumulative failure profile of the dtf particles in HRB-17/18 was a straight line or composed of straight line segments of high precision. The data shown in Fig. 3-2 do scatter rather widely but a straight line fit is also in order. The time probabilities of failure derived from the fits to the data of Fig. 3-2 are given by the values of the constant b of Table 3-2. Converting these b values to a per hour basis, the average value of b becomes 2.7/h. The average value of b observed for the HRB-17/18 experiment was 0.71/h close to 1/3 the value observed in the HFR-B1 experiment. In the latter, there were three fuel compact stacks compared to one in HRB-17/18 so that the

TABLE 3-1
 THE ESTIMATED VALUES IN EACH CAPSULE OF ^{85}mKr R/B FROM
 CONTAMINATION AND FROM FAILED, DESIGNED-TO-FAIL PARTICLES

	Mean Value of R/B ^(a) for Capsule:		
	A	B	C
$(\text{R/B})_c/10^{-6}$	5.79 • 0.57	6.04 ± 0.00	5.07 ± 1.54
No. of data used: first	4	1	3
$\text{R/B}_f/10^{-4}$	8.02 ± 0.42	8.92 ± 0.70	7.51 ± 1.13
No. of data used: last	3	4	5
$N_{\text{dtf}}^{(b)}$	1044	1044	1044

(a)The R/B values are based on the total fissile loading.

(b)The number of dtf particles per compact is now reported as 87 (Ke-87) and there are 12 compacts per capsule.

Ke-87 J. W. Ketterer "Fuel Loadings in Capsule HFR-B1 Fuel Compacts," GA Internal Memorandum, CED:435:JWK:87, July 23, 1987.

TABLE 3-2
 CALCULATION OF THE CUMULATIVE NUMBER OF FAILED
 DTF PARTICLES AT THE TIMES OF R/B MEASUREMENTS
 IN CAPSULE A, B AND C

Capsule	Date & Time	h	$\Delta t(d)$	N_f	a(a)	b(1/d)(a)
A	09.04.87 13.42	13.7	0	0		
	14.04.87 11.39	11.65	4.91	142		
	21.04.87 11.08	11.13	11.89	315		
	23.04.87 09.21	09.35	13.82	504		
	26.04.87 12.50	12.83	16.96	485		
	02.05.87 09.25	09.42	22.82	993		
	03.05.87 10.10	10.17	23.85	1030		
	04.05.87 13.30	13.50	24.99	1095		
					-206.	50.4
B	13.04.87 14.55	14.92	4.05	11		
	16.04.87 23.14	23.23	7.40	101		
	17.04.87 14.32	14.53	8.03	122		
	22.04.87 10.45	10.75	12.88	762		
	27.04.87 11.45	11.75	17.92	913		
	29.04.87 10.45	10.75	19.88	1072		
	02.05.87 20.11	20.18	23.27	942		
	03.05.87 18.30	18.50	24.19	1005		
04.05.87 12.30	12.50	24.95	1130			
					-356(b)	72.9(b)
C	16.04.87 22.07	22.12	7.35	52		
	21.04.87 16.20	16.33	12.11	594		
	24.04.87 10.03	10.05	14.84	591		
	28.04.87 17.12	17.20	19.15	883		
	30.04.87 09.00	9.00	20.80	1077		
	01.05.87 22.44	22.73	22.38	1093		
	03.05.87 02.49	2.82	23.55	810		
	04.05.87 02.19	2.32	24.53	1234		
	04.05.87 10.41	10.68	24.87	971		
					-393(c)	69.5(c)

(a) Coefficients in the time profile of the cumulative number of failed dtf particles: $N_f = a + bt(d)$ where N_f is the cumulative number of failed particles.

(b) Coefficients determined from data including the last three values of the couple (N_f , Δt).

(c) Coefficients determined from data including the last four values of the couple (N_f , Δt).

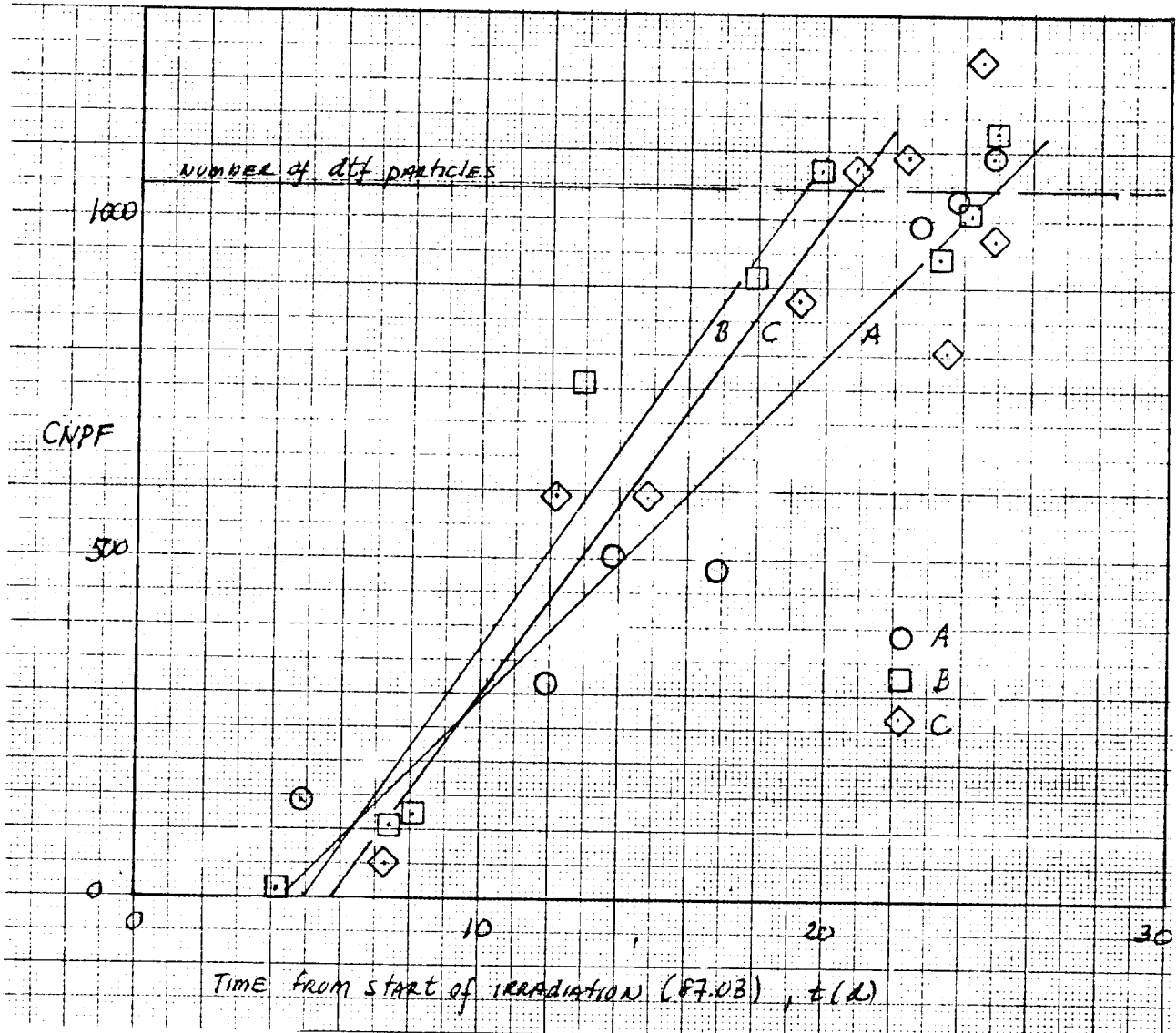


Fig. 3-2. The cumulative number of particles (dtf) failure as a function of time from start of irradiation

probability of the failure of a dtf particle in both experiments was comparable. Note that the length of the stacks were different in the two experiments, but this is not relevant to the foregoing comparison as long as the neutron flux and its axial variation are comparable in the two experiments.

The values of the constant b of Table 3-2 are proportional to the neutron fluence and flux, increasing with increase in the latter. Thus, the probability of failure increase with increasing neutron flux or fluence. On the basis of this correlation, no choice can be made among the thermal and fast neutron flux or fluence as to the failure inducing mode.

Data on the failure times, fast neutron fluxes, and fission rate densities applying to the dtf particles in experiments HRB-17/18 and HFR-B1 are presented in Table 3-3 (a). From the data in this table, one can show that (a) the fast fluence at the completion of the failure of dtf particles is three times greater in HFR-B1 than in HRB-17/18 and (b) that the number of fissions per unit volume of fissile fuels at the completion of failure is roughly the same in HFR-B1 and HRB-17/18. The specific values of the involved quantities are presented in Table 3-3 (b). These results indicate that the fast fluence is not involved in the failure, but that the failure is related to the number of fissions occurring. This conclusion is consistent with the previous analysis of the failure of dtf particles in HRB-17/18. For that experiment, the suggestion was made that fission fragment damage in the thin pyrocarbon coating of the dtf particles was responsible for the failure. This suggestion applies as well to HFR-B1 results.

The absolute ^{value} ~~view~~ of the R/B per failed dtf particle may be computed from the data of Table 3-1 on the assumption that the R/B values in this table are based on fissile loadings and on the fraction of dtf (fissile) particles present. The average value and standard deviation

TABLE 3-3(a)
 FAILURE TIMES OF THE DESIGNED-TO-FAIL (dtf) PARTICLES,
 FAST FLUENCES AND FISSION RATE DENSITIES FOR EXPERIMENTS
 HRB-17/18 AND HFR-B1

Exp/Capsule	Failure (h)		Δt (h)	Fast Flux (n/m ² .s)	Mean Fission Power(W) ^(a)	Fission Rate Density ^(b) (Fissions/m ³ .s)
	Start	End				
HRB/17	18.5	66.5	48	4.6E+18	-	1.5E+21
HRB/18	22.6	56.0	33	4.6E+18	-	1.5E+21
HFR-B1/A	98	595	497	1.6E+18	847	1.0E+20
/B	117	461	344	1.9E+18	1024	1.1E+20
/C	136	496	360	1.4E+18	876	9.7E+19

(a)The average of the fission power per capsule at the beginning and at the end of cycle 87.03.

(b)In converting from fission power per capsule to fission rate density (a) the equivalent numbers of compacts per capsule for capsules A, B and C were taken to be 12.0, 12.8 and 12.8, respectively, (b) the volume of the fissile ~~(normally configured and dtf) particles~~ was $2.06E-08 + 1.9E-09 = 2.25E-08$ m³ and (c) the number of fissions/J was taken to be $3.2E+10$ (based on 194 MeV/fission).

TABLE 3-3(b)
 FAST FLUENCE AND FISSION DENSITY AT COMPLETION OF DTF
 PARTICLE FAILURE IN EXPERIMENTS HRB-17/18 AND HFR-B1.

Experiment	Fast Fluence (n/m ²)	Fission Density (fissions/m ³)
HRB-17/18	1.0E+24	7.9E+27
HFR-B1	3.1E+24	4.5E+27

kerneles (from normally configured and dtf particles) per compact

[MM-100-WORMM]

of the $^{85}\text{m Kr}$ R/B for a failed dtf particle is calculated to be $(9.2 \pm 0.8) \cdot 10^{-3}$. This contrasts with the value of $4.8 \cdot 10^{-3}$ deduced from the HRB-18 experiment just after completion of dtf particle failure. The former value ^{of R/B} corresponds to a graphite temperature of about 870°C and ~~for~~ the latter value ^{to ABOUT} 770°C . The fuel temperatures ^{ARE} estimated to be 150°C higher. Combining the R/B ^{VALUES} with the temperature data permits an estimate of the activation energy for R/B to be made; thus, $Q/R = 10^4$ K. This compares with the standard value of 6400 K. Thus, one suspects the R/B derived from the HFR-B1 experiment to be somewhat higher than that applying to the HRB experiment for reasons other than temperature. ^{DEPENDENCE} Nevertheless, the mean values of R/B found near the end of cycle 87.03 indicate that the failure of the dtf particles is complete. This conclusion is strengthened by the initial R/B values found in the early stages of the subsequent cycle 87.05.

4. TRANSPORT OF GAS FROM CAPSULE TO SAMPLING VOLUME

4.1. INTRODUCTION

In the HFR-B1 experiment, the gas transport from the capsule to the sampling volume is reported in technical note P/F1/87/5. The gas flow lines are shown in Fig. 4-1. Table 4-1 shows the transit times for various flow rates and line volumes. Two questions concerning these data are:

1. Is the transient time given in columns 2, 3, and 4 that from the capsule exit to the sampling volume?
2. Do the decay volumes given in the headings of columns 3 and 4 represent decay tank or decay tank plus filter tank and ordinary tubings (for example, the tubing between MV32 and CV31 for the case of passage through DT3 only)? In any case, what volume is attributed to the tanks themselves and to the connecting tubing?

It is clear from the transit times in columns 2, 3, and 4 that slug flow is assumed; thus,

$$t = V/f_r \quad . \quad (4-1)$$

where t = transit time (min),
 v = volume of lines (cm^3),
 f_r = flow rate (cm^3/min).

However, the decay tanks will cause mixing of the successive volume elements of the slug flow and consequently a longer delay. If a well mixed

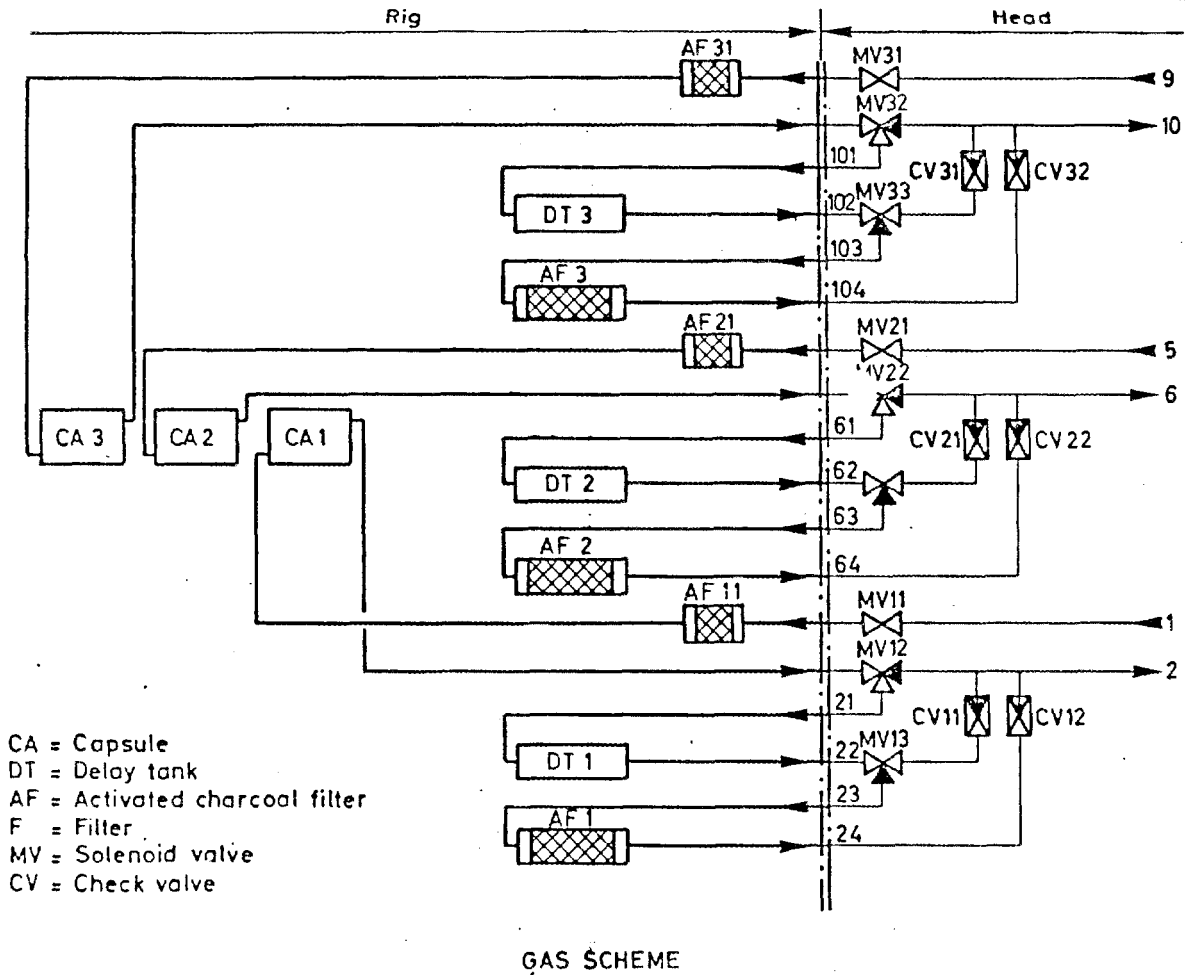


Fig. 4-1. Gas scheme of irradiation rig including rig head (taken from P/F1/87/5)

TABLE 4-1
 TRANSPORT TIMES OF DOWN-STREAM SWEEP GAS
 FOR DIFFERENT DECAY VOLUMES

Sweep Gas Mass Flow cm ³ min ⁻¹	Without Decay Volume 150 cm ³	Transport Times in Minutes Decay			In Capsule 100 cm ³
		Volume 360 cm ³	720 cm ³		
500	0.3	1	1.7	0.2	
300	0.5	1.7	2.9	0.3	
100	1.5	5.1	8.7	1	
50	3	10.2	17.4	2	
20	7.5	25.5	43.5	5	

volume is assumed, then for a delay tank volume of V_h (i.e., hold up volume) the transit time becomes

$$t = -(V_h/f_r) \ln (1-g) \quad ,$$

where g is the fraction of gas that has passed through volume V_h . Suppose that 90% of the gas has passed through volume V_h , then the transit time is

$$t = 2.3 V_h/f_r \quad . \quad (4-3)$$

Consequently, the transit time is 2.3 times longer for 90% of the gas to pass through a well mixed volume than for all of the gas to pass through a tubular segment of the same volume.

4.2. ANALYSIS OF THE GAS TRAIN

The transit time in the tubular segment of the gas train will be described by using Eq. 4-1. The further assumption in using Eq. 4-1 is no distortion of the time profile of gas concentration during tubular flow.

A more detailed analysis of the effect of the hold up volume on the gas profile is required as two factors enter here: the distortion of the profile and the delay of the gas element. Also, recognition is required of the differential nature of the experiment, i.e., measurements of a steady-state fractional gas release are of interest as contrasted to postirradiation experiments in which the profile of the cumulative gas release is of interest. Thus, let $A(t)$ be the density of atoms in the hold up volume V_h , then

$$\frac{dA(t)}{dt} = P(t) - (L + \lambda) A(t) \quad , \quad (4-4)$$

[MM-100-WORMM]

where $A(t)$ = density of atoms in V_h (atoms/cm³),
 $P(t)$ = inflow rate (atoms/cm³ · s)
 L = outflow frequency (1/s),
 λ = decay frequency (1/s).

Equation 4-4 yields

$$A(t) = A^0 e^{-(L + \lambda)t} + e^{-(L + \lambda)t} \int_0^t P(\tau) e^{(L + \lambda)\tau} d\tau, \quad (4-5)$$

where A^0 is the initial gas density in V_h .

To account for the effect of the hold up volume, the differential inflow and outflow must be comparable, thus

$$\frac{\partial P_r(t)}{\partial t} = P(t) \quad (4-6)$$

and

$$\frac{\partial R(t)}{\partial t} = LA(t) \quad (4-7)$$

where $P_r(t)$ is the time integral inflow to the well mixed volume and $R(t)$ is the response of the inflow profile to the effects of the well mixed volume. If

$$P(t) = K_1 + K_2 t, \quad (4-8)$$

where

$$K_i = \text{constant for } i = 1, 2,$$

then the case of a constant inflow ($t = 0$) and a rising or falling inflow rate ($K_2 > 0$, $t \neq 0$ or $K_2 < 0$, $t \neq 0$) can be treated.

Equation 4-7 becomes

$$LA(t) = LA^0 e^{-(L + \lambda)t} + \frac{K_1 L}{L + \lambda} \left\{ 1 - e^{-(L + \lambda)t} \right\} + \frac{K_2 L}{L + \lambda} \left\{ t - \frac{(1 - e^{-(L + \lambda)t})}{L + \lambda} \right\}. \quad (4-9)$$

If $t \gg (L + \lambda)^{-1}$, then

$$LA(t) = \frac{L}{L + \lambda} \left\{ K_1 + K_2 t \right\}. \quad (4-10)$$

In this case, the inflow rate can be obtained from the outflow rate by the relation

$$\frac{L + \lambda}{L} \left(\frac{\partial R}{\partial t} \right) = \frac{\partial P_r}{\partial t}. \quad (4-11)$$

If both sides are multiplied by the flow rate, f_r , then the right side of Eq. 4-11 represents the fission gas release rate, atoms/s, from the capsule in the absence of delay in the tubular segment of the gas train preceding the hold up volume. Thus, the reported steady-state fission gas release can be corrected by using the factor $(L + \lambda)/L$. The assumption of $t \gg (L + \lambda)^{-1}$ leading to this correction factor is justified below.

4.3. APPLICATION OF ANALYSIS TO THE HFR-B1 MEASUREMENTS

If the steady-state fractional release measured at the sweep gas sampling station is $(R/B)_S$, then the R/B at the capsule exit is

$$(R/B) = \prod_{n=1} \left(1 + \frac{\lambda}{L}\right)^n C^{-\lambda \sum V_i / f_r} (R/B)_S, \quad (4-12)$$

where V_i = tubular segment volumes in the gas train,
 n = number of well mixed volumes in the gas train,
 $L = f_r / V_h$.

To apply Eq. 4-12 requires information not presently available to the writer. Nevertheless, examining the factor $(1 + \lambda/L)$ is instructive. In particular, consider the ratio

$$R_f = \left(1 + \lambda/L\right) / e^{-\lambda/L} = \left(1 + \frac{\lambda}{L}\right) e^{\lambda/L}. \quad (4-13)$$

This represents the ratio of the $(R/B)_S$ correction factor for passage through a well mixed volume to that for passage through a tubular segment of the same volume. Assume values of 360 and 720 cm³ for a V_h and values of 50 and 300 cm³/min for the flow rate. Then the R_f values are shown in Table 4-2. At a flow ratio of 300 cm³/min, no account need be taken of the mixing in the decay tank or in the filter tank with respect to the decay of the radioactive isotopes. However, if the flow rate is reduced to 50 cm³/min, then account of the mixing in these tanks should be taken in correcting for the decay of the isotopes.

In applying the correction factor for the effects of the hold up volume, the assumption of $t \gg (L + \lambda)^{-1}$ was necessary. As the value of $L \geq 0.0012/s$ for the cases considered ($V_h \leq 720$ cm³, $f_r \geq 50$ cm³/min), the maximum value of $(L + \lambda)^{-1}$ is 14 min. Therefore, the inequality is satisfied for times greater than 1 h. Significant changes in the majority of the data occur over longer time periods and, therefore, the

[MM-100-WORMM]

assumption is justified in most cases. Analyses of more rapid changes in gas release should be treated in each case individually, if necessary.

TABLE 4-2
 THE RATIO, R_f , OF THE $(R/B)_s$ CORRECTION FACTOR FOR
 PASSAGE THROUGH A WELL-MIXED VOLUME TO THAT FOR PASSAGE
 THROUGH A TUBULAR SEGMENT OF THE SAME VOLUME

Isotope	Flow Rate (cm ³ /min)	R_f		$\lambda(1/s)$
		V_h	$2V_h$	
85mKr	300	1.01	1.01	4.30E-05
87Kr		1.02	1.04	1.51E-04
88Kr		1.01	1.02	6.73E-05
133Xe		1.00	1.00	1.53E-06
135Xe		1.00	1.01	2.11E-05 ^(a)
85mKr	50	1.04	1.08	
87Kr		1.14	1.29	
88Kr		1.06	1.12	
133Xe		1.00	1.00	
135Xe		1.02	1.04	

(a) Assuming the Xe-135 to be out of the irradiation field.

5. THE DETERMINATION OF HYDROLYSIS PRODUCT CONCENTRATIONS FROM GAS CHROMATOGRAPHIC MEASUREMENTS ON SAMPLES OF OUTLET GAS FROM CAPSULE C

Samples of outlet gas from capsule C during and after the first two water vapor injection tests were measured gas chromatographically for the presence of H₂, CO, CO₂, CH₄, O₂, and N₂. These measurements were not without difficulty and the problems will be discussed here. The first water vapor injection test (16.06.87; 1030 to 1644) will be treated first.

The calibration data applicable to the first test are presented in Table 5-1. The measurements of H₂, CO, and CO₂ in the gas samples of the first test are presented in Table 5-2. The following problems or peculiarities exist for these measurements:

1. The values of the ppmv associated with the first eleven rows of Table 5-2 are not the values obtained from the original chromatograms. Mr. Timke drew my attention to an error in these values that, as I remember, could roughly be corrected by multiplying by 1/2. However, after forming a table (Table 5-1) of the calibration data and using the factor from the calibration appropriate to the first eleven rows of data in Table 5-2, i.e., the calibration of 09:47:27, I found the areas listed in Table 5-2 multiplied by these factors yielded about the expected values of ppmv based on the rough correction stated above. Furthermore, the average of the set of ppmv values (see below) selected from the first eleven entries for hydrogen were in agreement with the average of the 12 and 13th row entries for hydrogen for which there is no question of the proper calibration factor. I do not understand this

TABLE 5-1
 CALIBRATION OF GAS CHROMATOGRAPH BEFORE, DURING AND
 AFTER THE WATER VAPOR INJECTION TEST

Day Time	GC Time	GC Area	Species	Conc (ppmv)	Factor
87/06/16 09:47:27	1.77	6675	CO ₂	51.9	7.78E-03
	2.43	6791	H ₂	48.3	7.12E-03
	2.90	1695	O ₂	41.2	2.43E-02
	3.54	5592	N ₂	37.8	6.75E-03
	4.49	16350	CH ₄	51.9	3.18E-03
	6.29	7254	CO	60.7	8.37E-03
87/06/16 13:29:45	1.78	7578	CO ₂	100	1.32E-02
	2.44	7857	H ₂	101.4	1.29E-02
	2.91	1989	O ₂	38.2	1.92E-02
	3.56	7675	N ₂	176.4	2.30E-02
	4.50	20127	CH ₄	130.2	6.47E-03
	6.32	8640	CO	192.8	2.23E-02
87/06/16 13:38:15	1.78	7172	CO ₂	94.7	1.32E-02
	2.44	7456	H ₂	96.2	1.29E-02
	2.91	2658	O ₂	51.1	1.92E-02
	3.56	7416	N ₂	170.5	2.30E-02
	4.50	20192	CH ₄	130.7	6.47E-03
	6.32	7307	CO	163.1	2.23E-02
87/06/16 13:49:23	1.78	8645	CO ₂	48	5.55E-03
	2.44	9034	H ₂	49	5.42E-03
	2.92	1915	O ₂	47	2.46E-02
	3.56	9005	N ₂	50	5.21E-03
	4.51	20004	CH ₄	52	2.60E-03
	6.32	9189	CO	48	5.22E-03
87/06/16 19:49	1.76	410	CO ₂	47.8	1.17E-01
	2.43	2062	H ₂	43.5	2.11E-02
	2.9	6083	O ₂	47.7	7.84E-03
	3.54	2169	N ₂	50.2	2.31E-02
	4.48	3880	CH ₄	51.1	1.32E-02
	6.31	293	CO	49.9	1.70E-01

TABLE 5-2
 DATA ON THE GAS CHROMATOGRAM AREA AND CONCENTRATION OF THE HYDROLYSIS
 PRODUCTS H₂, CO AND CO₂ BEFORE, DURING AND AFTER THE FIRST WATER
 VAPOR INJECTION TEST. ALL DATA ARE FOR 87/06/16

Cal	Time	H ₂		CO		CO ₂	
		Area	ppmv	Area	ppmv	Area	ppmv
09:47:27	1034	112139	798	77224	646	1563	12
	1045	18832	134	281	2.4(c)	1894	15
	1102	39128	279	36933	309	3163	25
	1111	{15117}(a) {28135}	{108}(a) {200}	382	3.2(c)	473	4
	1128	32495	231	24856	208	22766	177(d)
	1139	{4509}(a) {49840}	{32}(a) {350}	190	1.6(c)	26198	204(d)
	1150	19011	135	296	2.5(c)	1248	10
	1200	{7457}(a) {8141}	{53}(a) {58}	28830	241	13621	106(d)
	1212	25467	181	19800	166	1475	11
	1246	40810	291	21291	178	5468	43
↓	1306	39444	281	29044	243	33160	258(d)
13:49:23	1425	54624	296	56570	295	54300	302(d)
	1433	31677	172	{5571} {25920}	{29} {135}	4158	23
	1459	7406	40	1320	7	5065	28
	1509	20833	113	1284	7	6711	37
	1519	7870	43	18548	97	5632	31
	1527	7870	43	58195	304	5520	31
	1527	15783	86	93598	489	5765	32
	1546	7753	42	1461	8	4737	26
	1603	23121	125	45408	237	4748	26
↓	1630	11841	64	35774	187	8710	48

TABLE 5-2 (Continued)

Cal	Time	H ₂		CO		CO ₂	
		Area	ppmv	Area	ppmv	Area	ppmv
19:49	2029	(1232)(b)	26	ND	0.0	ND	0.0
	2048	(1137)(b)	24	ND	0.0	ND	0.0
↓	2103	(1185)(b)	25	ND	0.0	ND	0.0

(a)The central mark that appeared on all other chromatograms checked for number and location of marks (the first eleven listed for H₂) was missing for these traces.

(b)These areas were computed from the known factor. See Table 5-1.

(c)For all other chromatograms checked for letters following the area number (the first eleven listed for CO), the letter V followed the area number.

(d)In the case of these chromatograms, a center mark was absent.

complicated matter, but I accept the results, at least momentarily.

2. Among the first eleven entries for hydrogen, there are three occasions on which double measurements were repeated. In these cases, a central mark (a short line extending downward from the chromatogram curve, and, so far as I know, related to integration procedures in the GC equipment) was present and presumably resulted in integration over part of the hydrogen peak as evidenced by the generally lower area values as compared to the other measurements. The values of ppmv for the three occurrences of double measurements have been excluded from the data set considered in Section 2.
3. The first listed value of ppmv for hydrogen is sufficiently different from the other values so that it is excluded on a statistical basis.
4. The values of ppmv for the first twelve CO entries of Table 5-2 are "self-divided" into two groups: one with very low values, the other with values consistent with the H₂ values (see Section 2). From the records of the chromatogram, this distinction exactly correlates with the presence of the letter V following the printing of the number representing the area of the measured peak for the higher value group. The V, according to the GC manual, is connected with the second curve, unresolved peak. I did not study the manual well enough to understand this. However, I did trace the chromatogram curves in the vicinity of the CO peaks on four cases as shown in Fig. 5-1. (The traces shown have been enlarged in the process of reproduction.) These curves, especially the peaks, are visually similar and provide no justification for the enormous disparity in the corresponding concentrations (ppmv) reported by the GC computer. In fact, a rough

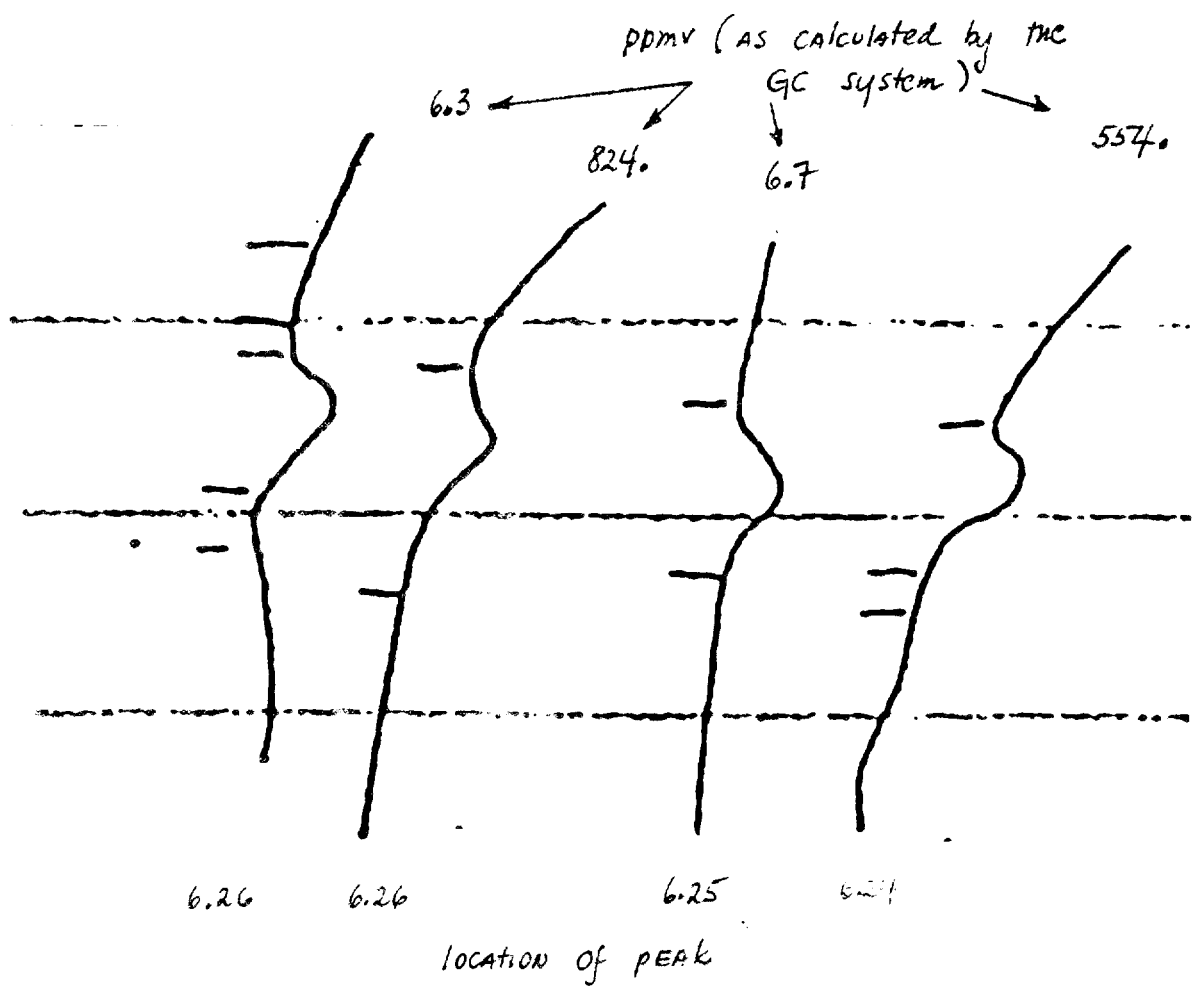


Fig. 5-1. Gas chromatograms in the vicinity of the CO peaks

measurement of the areas of the four peaks indicates an average value (on an arbitrary scale) of 65 ± 6 , i.e., the variation in areas of the four peaks of Fig. 5-1 is represented by a standard deviation of only 10%. Apparently then, the association of the letter V with many of the GC areas indicates that the peaks of Fig. 5-1, for example, are treated as the "second curve, unresolved peaks" by the GC machinery. Thus, in the set of the very low ppmv values, the measured "peak" must be a first curve - resolved peak. The only indication I find in the traces of Fig. 5-1 for a first curve is by treating the marks (the short, more or less horizontal segments on the left side of the curves) as indicators of integration limits. Then, for the first curve on the left, the interval between marks just prior to the major peak of this curve would delimit an area, roughly triangular in shape which might be treated by the GC as an area to be measured. If this happened, an area would be found such that the ratio of the area of the major peak to this peak is approximately 100; in fact, this is the ratio of the average area for the set of higher value concentrations to that for the set of lower value concentrations of CO given in Table 5-2 for the first twelve entries. Unfortunately for this hypothesis, there is no set of comparable marks setting off a small peak preceding the major peak for the third curve from the left of Fig. 5-1 for which the GC computer also reports a very small concentration.

A similar variation in peak areas and concentrations occur for CO in the set of values starting at 1459 and ending at 1630. Unfortunately, I did not note any letters that might have appeared with the area numbers on the chromatograms so the same criterion as is implicit above is not available here to discriminate between reasonable and unreasonable values. However, the extreme variation of the values within short periods

of time (for example between 1546 and 1603) is likely to reflect GC problems.

In any event, there is a clear need for careful monitoring and operation of the GC. Perhaps with a person more knowledgeable than I am about the GC, the problem of integration of the correct areas can be avoided.

5. A problem similar to the problem discussed in paragraph 4 occurred for the CO₂ determinations. The set of higher value concentrations (see Table 5-2) are from those chromatograms in which a mark was absent. In this case, however, the judgement was made that set of higher values is in error and that the lower value set is correct.

The analysis of reaction products in the second water vapor injection test (20.06.87 - 1226 to 24.06.87 - 1130) was much less successful than in the first test. The few measurements made are assembled in Table 5-3. The problems that existed for these measurements are as follows:

1. On June 21, there were two activity alarms in the reactor building attributed to leaks in the gas sampling portion of the sweep loops of D214.01. As a consequence of this, the practice of storing the gas samples before gas chromatographic analysis was begun. In this way, the activity level of these samples could be reduced. There was also another advantage related to interference by neon in measurement.
2. Measurements on June 20, the day injection began, revealed little hydrogen. The chromatograms should be reexamined to understand this result.

TABLE 5-3
 DATA ON THE CONCENTRATION OF THE HYDROLYSIS PRODUCTS H₂
 AND CO MEASURED GAS CHROMATOGRAPHICALLY DURING THE
 SECOND WATER VAPOR INJECTION TEST

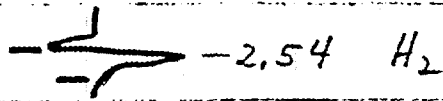
Sample Collection Time	Sample Measurement Time	Concentration (ppmv)	
		H ₂	CO
87.21.06 1245	87.22.06 1426	68	
		68	
		156	~33
		165	
		67	
87.22.06 1600	87.23.06 1122		19
		≥28	
87.24.06 1130	87.25.06 1505		4.3
			3.5
87.25.06 1015	87.29.06 ~1100	(a)	0

(a)H₂ peak masked.

3. During the gas chromatographic measurements for the second test, instances³ of massive interference of hydrogen peaks by neon were observed. Examples of a slight interference and a massive interference are shown in Fig. 5-2. The peak for hydrogen normally has its maximum at 2.44 (see Table 5-1). For the slight interference of Fig. 5-2, the peak has shifted to 2.54, although this is within the range observed in some other calibrations. Thus, one can be reasonably certain that the peak in the slight interference example is due to hydrogen although the peak area may be somewhat distorted due not only to neon interference, but also to the integration limits indicated by the marks. By contrast, the massive interference signal of Fig. 5-2, i.e., the negative going neon signal which is truncated at the left side of the GC recorder, completely masks the time interval during which hydrogen is normally being eluted. There is an unknown peak at 2.78, but between say 2.5 and 2.9 (the oxygen peak) there is no known signal for the calibration gas or the capsule effluent gas. Could it be that the hydrogen elution is retarded in the presence of neon and in the example of Fig. 5-2 is merely displaced? And if displaced, to what extent is it distorted? This seems an unlikely explanation. The acceleration of the oxygen elution is, a priori, an equally likely hypothesis as hydrogen retardation.

Clearly, the interference by neon is a major problem. In one case where the negative going neon signal occurred just before the hydrogen signal, helium (only) was swept through the sampling lines and into the GC with the result that the neon signal was reduced in the first gas chromatogram and did not appear on the second (see record of 87.06.73, 13:45:58, and 13.54:28). As there are common lines on the sweep loop used for the helium plus neon carrier gas in capsules A and B as well as pure helium carrier gas in capsule C, some

Slight INTERFERENCE



MASSIVE INTERFERENCE

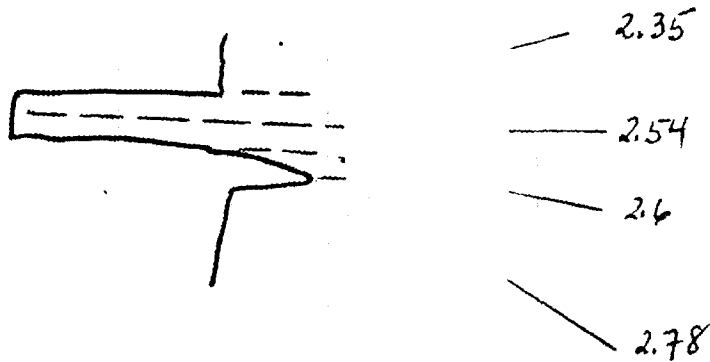


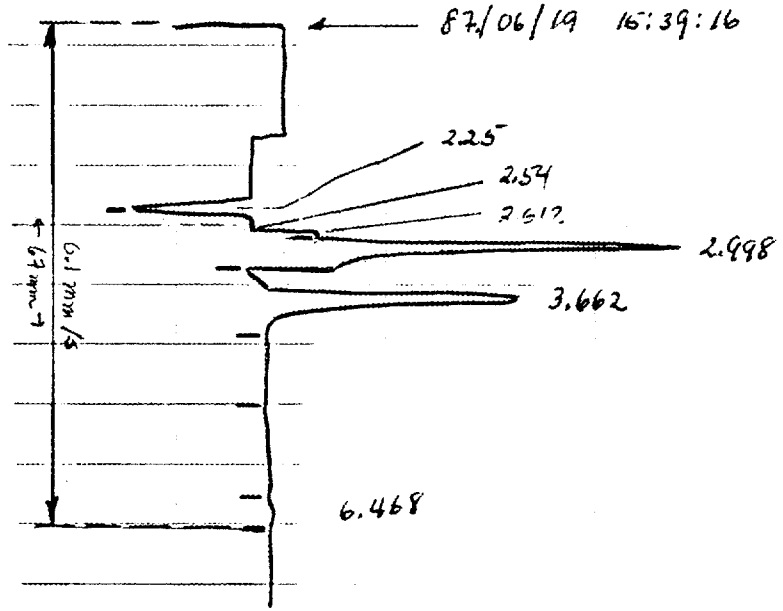
Fig. 5-2. Examples of the interference by neon in the gas chromatographic measurement of hydrogen

contamination of lines through which capsule C effluent passes can introduce neon into capsule C samples. A careful flushing of these common lines before sampling from capsule C will clearly aid in reducing neon contamination. However, this may not be the only source of neon contamination - a leak across closed valves is another source.

The simplest solution to the neon problem is to free the gas lines from capsule C to the sampling vial of neon by preventing leaks across valves and by flushing those lines. There are other, more complicated solutions such as (1) separating hydrogen from the gas samples and measuring hydrogen alone, (2) changing GC columns or altering conditions of elution (although this may not be possible), and (3) inverting the neon peak under conditions that the now negative going hydrogen peak can be seen as a perturbation.

4. The problem with integration of the area under the peaks of the chromatogram also was evident in the second water vapor injection test, but was complicated by the presence of neon. An example of this is shown in Fig. 5-3. Here, the profile of the chromatogram is similar in two cases; in the upper case, there is an extra integration mark and consequently an extra peak (H_2) is reported. This is very disconcerting to an analyst.
5. Finally, I address another problem with GC integration which involves the first five entries in column 3 of Table 5-2 for hydrogen. The traces of the corresponding hydrogen peaks are shown in Fig. 5-4. The mean of two of the five peak areas is, according to the gas chromatograph, 2.4 times the mean of the areas of the other three peaks. However, direct area measurements show that the variation among the peak areas is only 8%.

PEAK LOCATION	PEAK AREA	PPMV	
2.617	4134	68.2	H ₂
2.998	8009	54.4	O ₂
3.662	5258	85.0	N ₂
6.468	24	2.0	CO



PEAK LOCATION	PEAK AREA	PPMV	
2.998	21750	162	O ₂
3.658	8624	139	N ₂
6.625	1757	104	CO

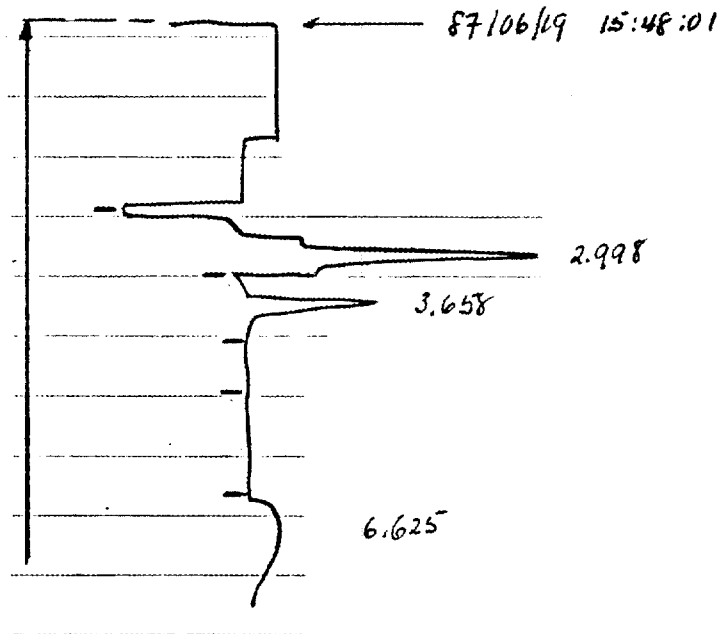


Fig. 5-3. Example of GC integration variation

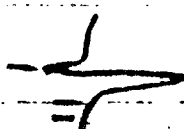
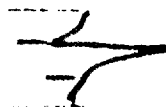
area	ppmv	
535	68.1 Hz	
534	67.9 Hz	
1228	156.3 Hz	
1298	165.1 Hz	
530	67.4 Hz	

Fig. 5-4. Repeated measurement by gas chromatography of the same gas sample

6. A SELF-TUTORIAL IN GAMMA SPECTROSCOPY

6.1. INTRODUCTION

In attempting to examine the raw data sheets obtained at Petten, it became necessary to understand the relations by which counting values are converted to steady-state fission gas release values. These relations were derived and are presented here chiefly for the benefit of the writer. Also, in order to analyze the data, the derivation of the R/B values must be thoroughly understood. Certain questions arise below the answers to which are necessary to complete this self-tutorial.

6.2. DERIVATION OF EXPRESSION FOR NUMBER DENSITY OF ISOTOPE IN SAMPLING VOLUME AT MOMENT OF COLLECTION

Let C be the total number of counts accumulated during the counting period, t_c (total live time) and let $\langle C_s \rangle = C/t_c$ be the count rate average (since the number of radioactive atoms declines during the counting period C_s is actually the average count rate). Then, the average concentration of atoms of a specific isotope present during the counting period is

$$\langle N_c \rangle = \frac{C}{t_c} \cdot \frac{e^{R\zeta}}{\epsilon b \nu \lambda} = \frac{C_s e^{R\zeta}}{\epsilon b \nu \lambda}, \quad (6-1)$$

where ϵ = detector efficiency,

b = branching ratio,

ν = sample volume,

λ = decay constant,

$e^{R\zeta}$ = correction factor for pulse pileup losses

R = total count rate for all isotopes,

ζ = amplifier pulse pileup time constant.

The average concentration of atoms of a specific isotope is also given by

$$\langle N_c \rangle = \frac{1}{t_c} \int_0^{t_c} N_0 e^{-\lambda t} dt \quad , \quad (6-2)$$

where

N_0 = number of atoms present at beginning of counting period.

Since a delay occurred between sampling and the start of counting

$$N_0 = N_\infty e^{-\lambda t_d}$$

where t_d is the delay time. Thus,

$$\langle N_0 \rangle = \frac{1}{t_c} \int_0^{t_c} N_\infty e^{-\lambda t_d} e^{-\lambda t} dt \quad . \quad (6-3)$$

Consequently,

$$\langle N_c \rangle = \frac{N_\infty}{\lambda t_c} e^{-\lambda t_d} (1 - e^{-\lambda t_c}) \quad , \quad (6-4)$$

and in combination with Eq. 1, yields

$$N_\infty = \frac{C_s t_c e^{R\zeta} e^{\lambda t_d}}{\epsilon \beta v (1 - e^{-\lambda t_c})} \quad , \quad (6-5)$$

where N_∞ is the number of atoms/cm³ present in the sampling volume at the moment of collection.

6.3. TOTAL COUNT RATES AND PULSE PILEUP LOSS CORRECTIONS

An estimate of the lower limit of the total count rate can be made as follows: Form the ratio $N_{\infty}'(t_{di})/N_{\infty}'(t_{d(i+1)})$; then, according to Eq. 6-5

$$\Delta R = R(t_{di}) - R(t_{d(i+1)}) = \frac{1}{\zeta} \ln \frac{N_{\infty}'(t_{d(i+1)})}{N_{\infty}'(t_{di})}, \quad (6-6)$$

where

$$N_{\infty}'(t_{dj}) = \frac{C_{stc} e^{\lambda t_{dj}}}{1 - e^{-\lambda t_c}} \quad (6-7)$$

If $\zeta = 5\mu s$, corresponding to a shaping time constant of $2\mu s$, then the minimum total count rate can be calculated for a sample measured at a series of delay times as shown in Table 6-1 for the data assembled in Table 6-2.

The data of Table 6-1 for the calculated, absolute minimum total count rate, $R_m = R_A - X$, can be represented quite well for krypton isotopes by the expression

$$R_m \text{ (counts/s)} = 2.518 E + 05 e^{-t_d \text{ (s)}/7213} \quad (6-8)$$

The characteristic decay time is essentially 2 h (7213 s). That the minimum calculated count rate is too high for accurate measurement at delay times of 2 h or less is clear from the data of Table 6-1 as well as Eq. 6-8. The values of R_A computed from xenon isotopes are in agreement with those based on the krypton isotopes only for Xe135; the uncertainty in the counting of Xe133 is apparently large enough to result in the scatter inherent in the R_A values for Xe133 listed in Table 6-1.

TABLE 6-1
 INCREMENTAL TOTAL COUNT RATES AT A SERIES OF DELAYS PRIOR
 TO GAMMA COUNTING THE FISSION GAS SAMPLE
 TAKEN FROM CAPSULE C AT 0049 ON JUNE 12, 1987

Spectrum	$t_d(s)$	$\Delta R(\text{Counts/s})$			$\langle \Delta R \rangle$	RA ^(a) (counts/s)
		^{85}Kr	^{87}Kr	^{88}Kr		
2294	3660	65700	59600	62000	62400	153300+X
2295	7260	51200	45850	46700	47900	87600+X
2296	14460	24300	24750	23250	24100	36400+X
2297	21660	12100	---	11000	11500	12100+X
2298	21660	X _{85m}	X ₈₇	X ₈₈	X	X
---	∞					

Spectrum	$t_d(s)$	$\Delta R(\text{counts/s})$	
		^{133}Xe	^{135}Xe
2294	3660	44600	63000
2295	7260	83400	52000
2296	14460	20700	23600
2297	21660	3250	---
2298	21660		

RA = The calculated absolute minimum

TABLE 6-2
 CALCULATION OF THE COUNT AND DELAY TIME CORRECTED NUMBER
 OF ACCUMULATED COUNTS FOR MEASUREMENTS ON A SAMPLE
 TAKEN FROM CAPSULE C AT 0049 ON JUNE 12, 1987

Isotope	Spectrum	$t_d(s)$	$t_c(s)$ (a)	$C_s(\text{counts/s})$	$C_s t_c e^{\lambda t_d} / (1 - e^{-\lambda t_c})$	$N_0 =$	Ratio
Kr85m	2294	3660	1925	195	5.53E+06		1
	2295	7260	1518	234	7.68E+06		1.39
	2296	14460	1268	223	9.92E+06		1.79
	2297	21660	1173	185	1.12E+07		2.03
	2298	28860	1121	145	1.19E+07		2.15
Kr87	2294	3660	1925	183	2.42E+06		1
	2295	7260	1518	147	3.26E+06		1.35
	2296	14460	1268	63	4.10E+06		1.69
	2297	21660	1173	24	4.64E+06		1.92
	2298	28860	1121	8	4.60E+06		1.90
Kr88	2294	3660	1925	206	4.10E+06		1
	2295	7260	1518	222	5.59E+06		1.36
	2296	14460	1268	172	7.06E+06		1.72
	2297	21660	1173	118	7.93E+06		1.93
	2298	28860	1121	76	8.38E+06		2.04
Xe133	2294	3660	1925	9.2	1.16E+07		1
	2295	7260	1518	4.6	1.45E+07		1.25
	2296	14460	1268	2.9	2.20E+07		1.90
	2297	21660	1173	2.0	2.44E+07		2.10
	2298	28860	1121	1.9	2.48E+07		2.14
Xe135	2294	3660	1925	108	1.08E+07		1
	2295	7260	1518	55	1.48E+07		1.37
	2296	14460	1268	26	1.92E+07		1.78
	2297	21660	1173	15.5	2.16E+07		2.00
	2298	28860	1121	13.4	1.96E+07		1.81

(a) Assumed to be the live-time counting period and not the real-time counting period.

Bearing on the total count rate, is the dependence of the corrected number of accumulated counts for specific isotopes as a function of the delay time between sample collection and measurement. This is shown in Fig. 6-1 for the data (N'_{∞} and t_d) of Table 6-2. In addition, some data from a sample taken from capsule C at 1410 on June 16, 1987, are included in Fig. 6-1; these data are presented in Table 6-3. In considering Fig. 6-1, note that

$$N_{\infty} = N'_{\infty} (e^{R\zeta}/\epsilon b\nu) \quad . \quad (6-9)$$

The derived value of N_{∞} should, in principle, be independent of t_d . Consequently, the multiplier of N'_{∞} in Eq. 6-9 would have to change with t_d . Only the factor $\exp(R\zeta)$ will change for a specific isotope. The change in $\exp(R\zeta)$ must occur in a manner that yields a constant value for the product $N'_{\infty} \exp(R\zeta)$, since this product is equal, aside from a constant, to the number of atoms, N_{∞} , present in the fission gas sample. This is possible, since R decreases with increasing t_d . Furthermore, it would appear from the data in Fig. 6-1 for each isotope that an asymptote is rapidly being approached at large t_d values and that this asymptote must be equal, aside from the constant $1/\epsilon b\nu$, to the value of N_{∞} . If an asymptote is being approached (neglecting measurement limitations that might prevent a true asymptote from being observed), then the value of X in Table 6-1 became negligible. In this event, the absolute values of the total count rate become known with a negligible error and the data of Fig. 6-1 can be corrected for the pulse pileup loss. This is shown in Fig. 6-1 for the isotope ^{85}mKr .

6.4. RATIO OF ATOMS AMONG ISOTOPES MEASURED

In spite of the large corrections to count data taken at short delay times, the underlying measurements are quite consistent as shown by the corrected data in Fig. 6-1 and the consistency of one of the factors as shown by Eq. 6-8 entering into the correction. Another indication of the underlying consistency, independent of the corrections

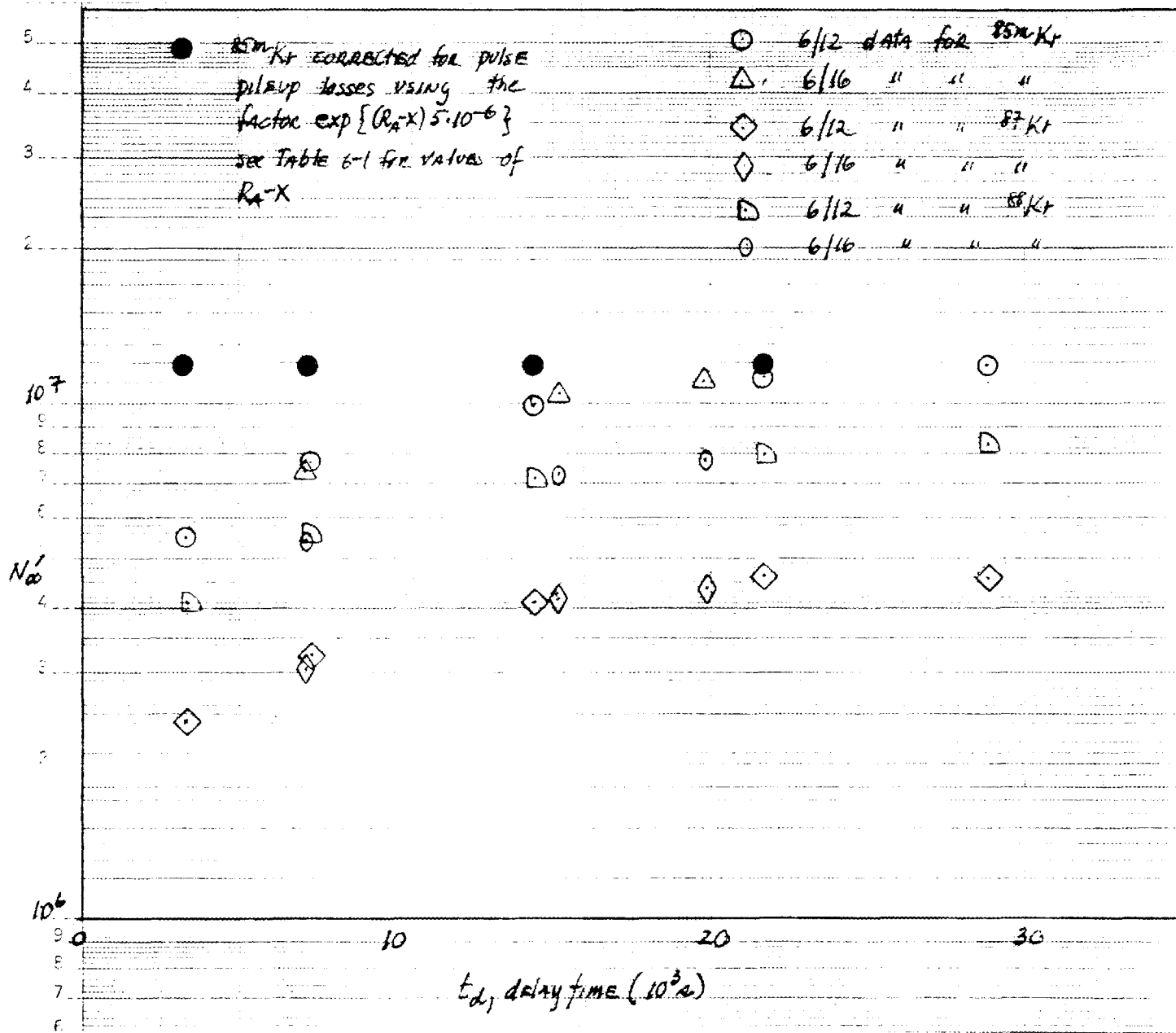


Fig. 6-1. The count- and delay-time corrected number of accumulated counts

TABLE 6-3
 CALCULATION OF THE COUNT AND DELAY TIME CORRECTED NUMBER
 OF ACCUMULATED COUNTS FOR MEASUREMENTS ON A SAMPLE TAKEN
 FROM CAPSULE C AT 1410 ON JUNE 16, 1987

Isotope	Spectrum	$t_d(s)$	$t_c(s)$ (a)	C_s	N_a
Kr85m	2365	7140	1596	227	7.43E+06
	2366	15120	1262	227	1.04E+07
	2367	19560	1196	201	1.11E+07
Kr87	2365	7140	1596	139	3.05E+06
	2366	15120	1262	58	4.18E+06
	2367	19560	1196	31	4.36E+06
Kr88	2365	7140	1596	209	5.24E+06
	2366	15120	1262	168	7.22E+06
	2367	19560	1196	132	7.69E+06

(a) Assumed to be the live-time and not the real-time counting period.

(which after all, are simply self consistent) is given by the ratio of atoms for each spectrum. Thus

$$\frac{[N_{\infty}]_i}{[N_{\infty}]_j} = \frac{[N_{\infty\epsilon b}]_i}{[N_{\infty\epsilon b}]_j} \quad , \quad (6-10)$$

where i and j represent different isotopes.

The relative values are shown in Table 6-4 based on data in Tables 6-2 and 6-5. The relative values of the number of atoms at the time the fission gas samples were collected, $[N_{\infty}]_i/[N_{\infty}]_{Kr85m}$ are constant with a fractional standard deviation of less than 0.07. There is apparently a small decrease in values with increasing time delays before counting, the origin of which is unknown.

TABLE 6-4
 THE RELATIVE NUMBER OF ATOMS OF SELECTED ISOTOPES
 IN THE FISSION GAS SAMPLE AT THE MOMENT OF COLLECTION

Spectrum	Relative No. of Atoms, $[N^i]_t / [N^{85m}]_{Kr85m}$ for $i =$					
	$t_d(s)$	^{85m}Kr	^{87}Kr	^{88}Kr	^{133}Xe	^{135}Xe
2294	3660	1	0.106	0.179	0.868	1.45
2295	7260	1	0.103	0.176	0.782	1.43
2296	14460	1	0.100	0.172	0.918	1.43
2297	21600	1	0.100	0.171	0.902	1.43
2298	28860	1	0.094	0.170	0.863	1.22
Mean Values		1	0.101	0.174	0.867	1.39
Standard Deviation		-	0.004	0.004	0.053	0.10
Fractional Standard Dev.		-	0.044	0.022	0.061	0.069

TABLE 6-5
 CONSTANTS AND PARAMETERS NEEDED IN CALCULATION OF THE
 NUMBER OF ATOMS OF AN ISOTOPE PRESENT IN A FISSION GAS SAMPLE

Isotope	b(a)	ϵ (b)	ϵb
^{85m}Kr	0.785	1.20E-03	9.42E-04
^{87}Kr	0.503	4.53E-04	2.28E-04
^{88}Kr	0.263	9.84E-04	2.59E-04
^{133}Xe	0.371	1.05E-03	3.90E-04
^{135}Xe	0.903	7.73E-04	6.98E-04

(a) Values taken from "Table of Isotopes, Seventh Edition" edited by C.M. Lederer and V.S. Shirley, John Wiley and Sons, Inc. 1978.

(b) Values taken from "IMGA Operating Manual" K.H. Valentine and M.J. Kania, ORNL/TM-6576, August 1979. Only the relative values of ϵ are used here as the absolute values listed apply to a specific source-detector geometry.

7. THE DETERMINATION OF R/B, COMPARISON WITH REPORTED VALUES AND DEPENDENCE ON DECAY CONSTANT (PARTIALLY A SELF-TUTORIAL)

As a measure of my understanding of the calculation of R/B under the Petten experimental conditions, an attempt is made here to calculate relative R/B values from the raw data obtained during my recent trip to Petten. The results are compared with the reported results. Some possible discrepancy exists between the compared data which will be understood only when the detector efficiencies for the Petten source-detector geometry are requested and received. The dependence of R/B on decay constant is also examined.

7.1. DETERMINATION OF R/B AND COMPARISONS

The R/B for an isotope is calculated according to the equation

$$R/B = \frac{Nf_r}{F_r Y} \quad , \quad (7-1)$$

where N = the number density of atoms released from the fuel elements (atoms/cm³),

f_r = flow rate (cm³/s),

F_r = fission rate (fissions/s),

Y = yield of a specific isotope.

Normally, the R/B is calculated at the time of release from the fuel element. This implies that the transit time, t_t^f , to the sample collection volume and the decay time, t_d , between collection and measurement have to be known. The correction for the transit time has been discussed in Section 4. Thus, the number density at the time of release

from the fuel element based on the number density at the start of the gamma counting period is given by

$$N = N_{\frac{t}{0}} e^{\lambda (t_d + t_f)} = N_{\infty} e^{\lambda t_f} \quad , \quad (7-2)$$

where $N_{\frac{t}{0}}$ = number density of atoms at the start of gamma counting (atoms/cm³),

N_{∞} = number density of atoms at the moment of sample collection (atoms/cm³).

The complete expression for the R/B corrected to the start of counting is

$$(R/B) = \frac{C e^{R\zeta} f_r}{\epsilon b \nu (1 - e^{-\lambda t_c}) F_r Y} \quad , \quad (7-3)$$

where C = number of counts during counting period,
 R = total count rate for all isotopes (counts/s),
 ζ = pulse pileup time constant (s),
 ϵ = detector efficiency,
 b = branching ratio for a specific isotope,
 λ = decay constant (1/s),
 t_c = counting time (live) (s).

Since the detector efficiencies are not available to me as of this writing, the relative R/Bs will be calculated. Thus, using Kr85m as the reference,

$$\frac{(R/B)_i}{(R/B)_r} = \frac{C_i}{C_r} \cdot \frac{\epsilon_r}{\epsilon_i} \cdot \frac{b_r}{b_i} \left(\frac{1 - e^{-\lambda_r t_c}}{1 - e^{-\lambda_i t_c}} \right) \frac{Y_r}{Y_i} \quad . \quad (7-4)$$

If the relative R/Bs corrected to collection of the sample or to release from the fuel elements are desired, then Eq. 7-4 is multiplied by either

$\exp \{(\lambda_1 - \lambda_r)t_d\}$ or $\exp \{(\lambda_1 - \lambda_r)(t_d + t_f)\}$, respectively. Since $t_d \gg t_f$ in the cases to be calculated, only the latter case will be considered in addition to the case of Eq. 7-4.

In calculating the relative R/Bs according to Eq. 7-4, the birth rate is based on all fissions occurring in both fissile and fertile fuel. What is desired is the birth rate in the designed-to-fuel (dtf) particles, at least, in the early stages of the experiment when failure of the normally configured fissile particles is unlikely. In any event, the fission rate in fissile particles must be known apart from the fission rate in fertile particles. Knowing the fission rate in the fissile particles, the fission rate in the dtf particles can be calculated from the ratio of the dtf to normally configured particles. At this time, I assume that the R/Bs reported from Petten are based on the total fission rate, that is, on fissile and fertile particles.

The values of the quantities in Eq. 7-4 are presented in Table 7-1. The values of ϵ_i are treated in the two following ways. A set of relative values is taken from the efficiency-energy curves applying to the source-detector geometries of the ORNL IMGA system. The curves for five geometries are shown in Fig. 7-1; that the relative efficiencies are sensibly constant among the different geometries can be seen from this figure. Using the curve marked 20 cm, the relative detector efficiencies, ϵ_i/ϵ_r where ϵ_r is the detector efficiency at 150 keV (^{85m}Kr), are 1, 0.38, and 0.82 for i representing ^{85m}Kr , ^{87}Kr and ^{88}Kr , respectively. The other approach to the detector efficiencies is by calculating the detector efficiencies required to match the R/B values reported from Petten.

One ambiguity in the data reported from Petten must first be resolved. By comparing the raw data, I received at Petten and the table of R/B data for capsule C, it is clear that the time quoted for the R/B values is the time at which the counting started. So the question arises: Are the R/B data corrected to the time at which counting

TABLE 7-1
 QUANTITIES NEEDED TO CALCULATE THE RELATIVE R/Bs FOR THE
 FISSION GAS SAMPLE TAKEN FROM CAPSULE C ON JUNE 15 AT 1105
 AND MEASURED AS SPECTRUM 2349

Quantity	85mKr	87Kr	88Kr
C_i (Counts)	341622	216628	324322
ϵ_i	(a)	(a)	(a)
b_i	0.785	0.503	0.263
λ_i (1/s)	4.30E-05	1.51E-04	6.73E-05
Y_i	1.31E-02	2.54E-02	3.58E-02
t_c (s) (b)	1493	1493	1493
t_d (s)	6900	6900	6900
$1 - e^{-\lambda_i t_c}$	6.22E-02	2.02E-01	9.56E-02
$e^{\lambda_i (t_d + t_f)}$	1.35	2.89	1.60
t_f (s) (c)	120	120	120

(a) See text.

(b) Assumes to be live time.

(c) Assumes a flow rate of 300 cm³/min and a decay volume of 360 cm³ in line from the release of gas in the fuel element to the collection of the gas samples in the sample volume. Thus according to Table 4-1, the transit time is 1.7+0.3 = 2.0 min (120 s). Note that the calculations in the text are not particularly sensitive to the value of t_f since $t_d \gg t_f$.

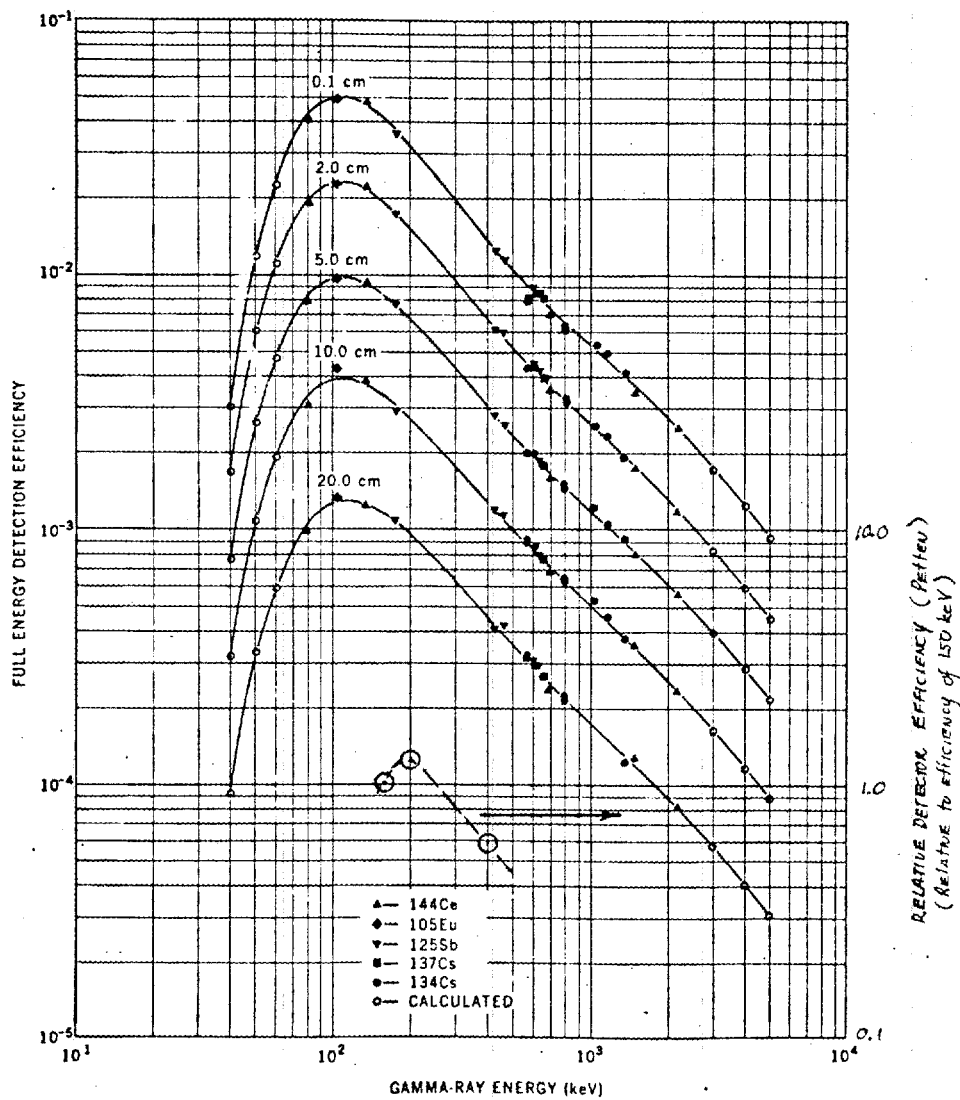


Fig. 7-1. Point-source, full-energy peak detection efficiency as a function of gamma-ray energy for five source-detector geometries of the IMGA system

started? I conclude that this is not so, for if the R/B data reported, for example, at 1300 on June 15th were corrected for the transit and decay times between gas release and the start of counting, the corrected R/B values would be abnormal. Thus, for the reputed values of R/B for ^{85m}Kr , ^{88}Kr , and ^{87}Kr , of $6.51 \text{ E-}04$, $4.14 \text{ E-}04$, and $3.81 \text{ E-}04$, one would obtain corrected values by multiplying by $\exp \{ \lambda_1 (t_d + t_f) \}$ (see Table 7-1) of $8.79 \text{ E-}04$, $6.62 \text{ E-}04$, and $1.10 \text{ E-}03$, respectively. A larger R/B for ^{87}Kr than ^{85m}Kr or ^{88}Kr has never been observed and makes no sense physically. Therefore, the conclusion is reached that the Petten reported R/B values apply to the time of gas release from the fuel element. The reporting of the time at which the gas sample left the fuel element or even the time of collection of the gas sample is preferable; otherwise, the time resolution of the release data is degraded by several hours.

The results of the calculations using Eq. 7-4 are presented in Table 7-2. It is quite clear that a large discrepancy exists between the calculated and reported relative R/B values. Thus, the relative detector efficiencies assumed in the calculation could be significantly in error. The relative detector efficiencies required to permit the correct relative R/B values to be calculated by using Eq. 7-4 are shown also in Table 7-2 and are plotted in Fig. 7-1 using the scale on the right hand ordinate. Note that the slope of the relative efficiency-energy curve for energies of greater than 200 keV is similar to those shown for the detector in the IMGA system, but that the peak in the efficiency-energy curve is shifted to a higher value by about 100 keV than the other curves shown. The actual detector efficiency values are eagerly awaited.

7.2. THE DEPENDENCE OF R/B OR RELATIVE R/Bs ON DECAY CONSTANT

The dependence of R/B or relative R/B values on decay constant is shown in Fig. 7-2 for data from the R2-K13 experiment and from the HFR-B1 experiment. The former data are absolute values of R/B obtained

TABLE 7-2
 THE CALCULATION OF RELATIVE R/B VALUES AND COMPARISON WITH
 REPORTED VALUES FOR THE FISSION GAS SAMPLE TAKEN FROM
 CAPSULE C ON JUNE 15 AT 1105 AND MEASURED AS SPECTRUM 2349

Relative (R/B) Values Corrected to Release From The Fuel
 Element and Relative Efficiencies

Isotope	$(R/B)_i / (R/B)_r$		Relative Efficiencies, ϵ_r / ϵ_i	
	Calc	Reported(a)	ORNL(b)	Petten(c)
^{85m}Kr	1	1	1	1
^{87}Kr	0.88	0.59	2.63	1.70
^{88}Kr	0.97	0.64	1.22	0.79

(a) Based on absolute R/B values reported by Petten of $6.51\text{E}-04$, $3.81\text{E}-04$ and $4.14\text{E}-04$ for ^{85m}Kr , ^{87}Kr and ^{88}Kr , respectively.

(b) From Fig. 7-1, the 20 cm geometry case.

(c) Required to satisfy Eq. 7-4 where $(R/B)_i / (R/B)_r$ are those deduced from the report values (see (a) above).

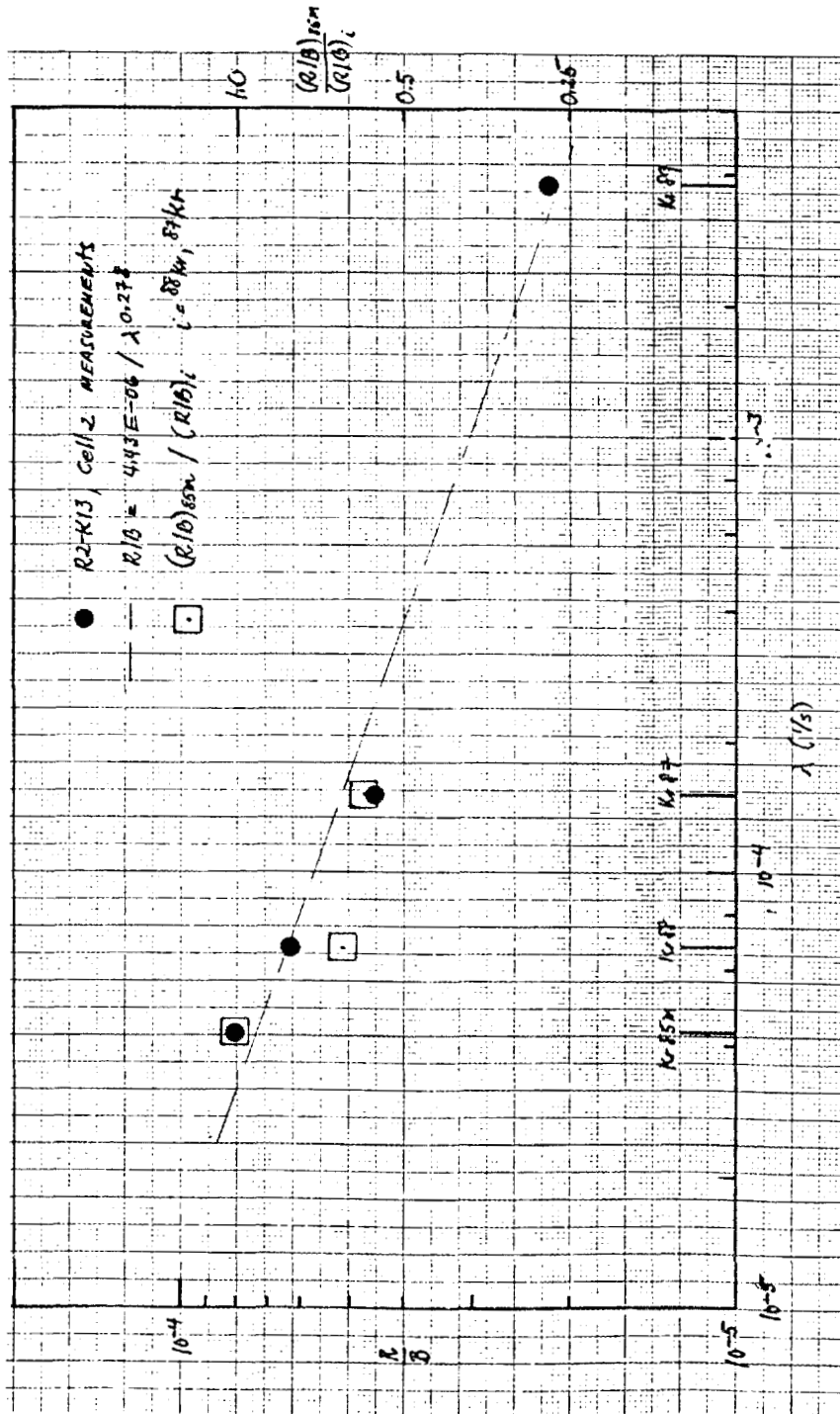


Fig. 7-2. Comparison of relative R/B values from capsule C of HFR-B1 (taken 6/15/87 at 1105: spectrum 2349) with R/B values from Cell 3 of R2-K13

from cell 2 at 1175°C and the latter values are relative values of R/B derived from the measured absolute values from capsule C on the sample taken at 1105 on June 15th and identified with spectrum 2349. Three features of this figure are noted: (1) the relative values of R/B for ^{85m}Kr and ^{87}Kr are similar in the two experiments, (2) the relative value (and consequently, the absolute value of R/B) for ^{88}Kr is abnormally low with respect to ^{85m}Kr in the HFR-B1 case and (3) the dependence of R/B on λ cannot be confidentially derived from R/B or relative R/B values only for ^{85m}Kr , ^{88}Kr , and ^{87}Kr .

That the R/B for ^{88}Kr derived from the HFR-B1 experiment is abnormally low in comparison to ^{85m}Kr and too small in comparison to that for ^{87}Kr is not only substantiated by comparison with data from R2-K13, but also with data from the GA TRIGA reactor and the ORNL HFIR reactor as, for example, in experiment HRB-17/18. There is a mechanism by which the R/B for ^{88}Kr would be smaller than expected on the basis of a linear relative between $\ln R/B$ and $\ln \lambda$. Under circumstances in which the release of krypton isotopes is governed by the release of the krypton precursor, bromine, the release of ^{88}Kr would be relatively low. This results from the relative half-lives of the bromine precursors: thus, the half-lives for ^{85}Br , ^{87}Br , and ^{88}Br are respectively 2.9 min, 56 s, and 17 s. In oxide fuels, the effect may not be masked by diffusion and release of the longer lived daughter, krypton, as a result of the diffusion coefficient of bromine which is 200 times larger than that of krypton in UO_2 .

In the case of gas release from contamination, where diffusion in UO_2 is not involved, the relatively low release of ^{88}Kr would not be expected; yet, from the earliest measurements in HFR-B1 before particle failure occurred and during the time governed by gas release from the fissioning of contamination, similar patterns of gas release among the three isotopes of krypton were observed.

It is important to understand at the outset of the HFR-B1 experiment why all the R/B measurements of ^{88}Kr are smaller than expected on the basis of experience in similar reactor experiments. The first effort on this matter ought to be the examination of all measurements and calculations associated with the R/B determination before embarking on further analysis of the data.

There is, of course, the smaller probability that the relative R/B values are too high for either $^{85\text{m}}\text{Kr}$ or ^{87}Kr , rather than being too low for ^{88}Kr . However, in either of these cases, the dependence on decay constant, after correcting for the hypothesized high values, would be either too small (for the case of a high relative R/B of $^{85\text{m}}\text{Kr}$) or too large (for the case of a high relative R/B of ^{87}Kr) compared to normally observed dependencies.

In regard to determining the dependence of R/B on decay constant, which is important in assessing the mechanisms of gas release, the data of Fig. 7-2 demonstrate via the R2-K13 data that using R/B values for the isotopes $^{85\text{m}}\text{Kr}$, ^{87}Kr , and ^{88}Kr , would yield a stronger dependence than is derived by including the R/B for the isotope ^{87}Kr in the calculation. Therefore, accurate values of the decay constant dependence of the R/B are not to be expected from most of the HFR-B1 data. However, using the R/B values for the three longer-lived krypton isotopes in the R2-K13 case, does appear to yield an upper limit to the strength of the dependence. In the case of the HFR-B1 data, given the present premise that the R/B for ^{88}Kr is low, the upper limit to the dependence of R/B on decay constant might be better estimated using only R/B values for $^{85\text{m}}\text{Kr}$ and ^{87}Kr .

After the above was written, I examined the R/B data for capsules A and B before any failure of the dtf particles and for measurements including the short-lived isotopes of ^{89}Kr and ^{90}Kr (data taken from R. Conrad's technical memorandum HFR/87/2380, 29.07.87). These data are shown on Fig. 7-3. It is clear from this figure that the R/B values for

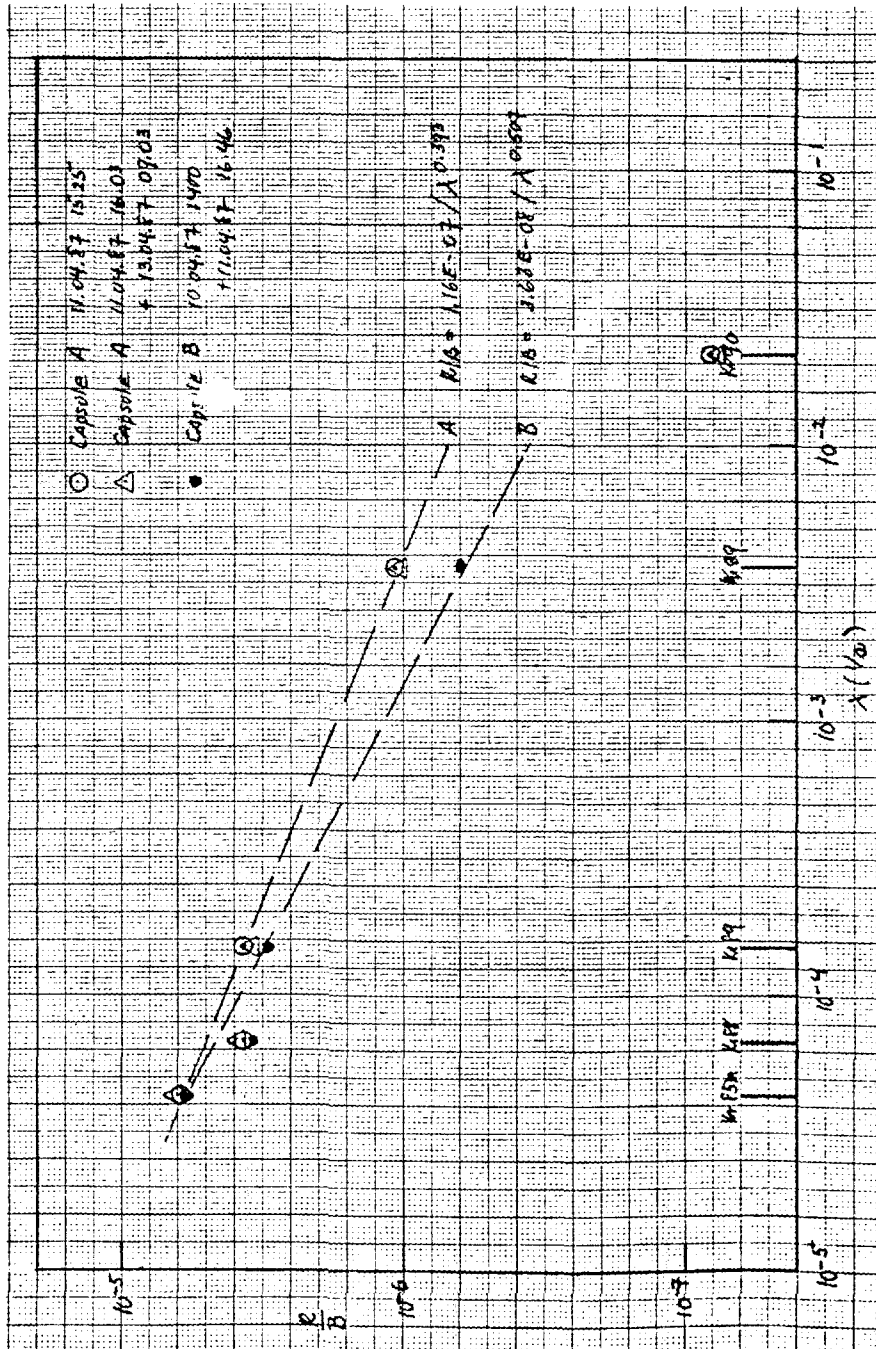


Fig. 7-3. The dependence of R/B on decay constant for fission gas release from capsules A and B before failure of dtf particles

[MM-100-WORMM]

^{85m}Kr , ^{87}Kr and ^{89}Kr satisfy the relation $R/B = A/\lambda^n$, where A and n are constants, quite well and that the R/B values of ^{88}Kr are definitely low by comparison. The ^{90}Kr R/B are also quite smaller than expected, but this can be attributed to a release time which is comparable to or larger than the decay time of the ^{90}Kr isotope (32.3 s).

8. DETERMINATION OF RELATIVE R/B VALUES FOR ^{85m}Kr FROM MEASUREMENTS DURING THE FIRST WATER VAPOR INJECTION TEST

The R/B value, corrected to the time of collection, is given by Eq. 7-3 of Section 7. Multiplied by $\exp(\lambda t_d)$ in order to correct for the decay between collection and measurement,

$$(R/B)_{\text{col}} = \frac{C e^{R\zeta} f_r e^{\lambda t_d}}{\epsilon b \nu (1 - e^{-\lambda t_c}) F_r Y} , \quad (8-1)$$

where all the symbols have been defined in Section 7, except for t_d which is the delay time between collection and the start of counting. the relative R/B values for a specific isotope can be derived from the quantity

$$Q = C e^{R(t_d)\zeta} e^{\lambda t_d} / (1 - e^{-\lambda t_c}) . \quad (8-2)$$

assuming the fission rate, F_r , to be approximately constant over the time of the test. To calculate Q values, the data of Table 8-1 are used plus the following expression and values:

$$R(t_d) = 2.518 E + 05 e^{-t_d(s)/7213} , \quad (8-3)$$

which is Eq. 6-8 of Section 6 and $\zeta = 5 \mu\text{s}$ and $\lambda = 4.3 E - 05/\text{s}$. the values of Q are given in Table 8-1.

TABLE 8-1
 DATA TAKEN FROM THE RAW GAMMA COUNTING RECORDS
 (SEE SECTION 9) AND CALCULATION OF THE ISOTOPE
 SPECIFIC QUANTITY Q (SEE EQ. 8-2)

Day	Collection Time	Spectrum	t_d (s)	t_c (s)	C_1 Counts	Q
15	1105	2349	6900	1493	341622	1.20E+07
16	0842	2362	7200	1493	339026	1.18E+07
16	1418	2366	15120	1262	286217	1.21E+07
16	2100	2369	11040	1435	385432	1.36E+07
17	1710	2379	21600	1195	248331	1.34E+07
18	1300	2389	21600	1187	235332	1.28E+07
19	1100	2399	18900	-(a)	251236	1.20E+07
20	0936	2409	6840	1488	331894	1.17E+07

(a)Used value of 1237s based on fit of t_c versus t_d data as shown in Fig. 8-1.

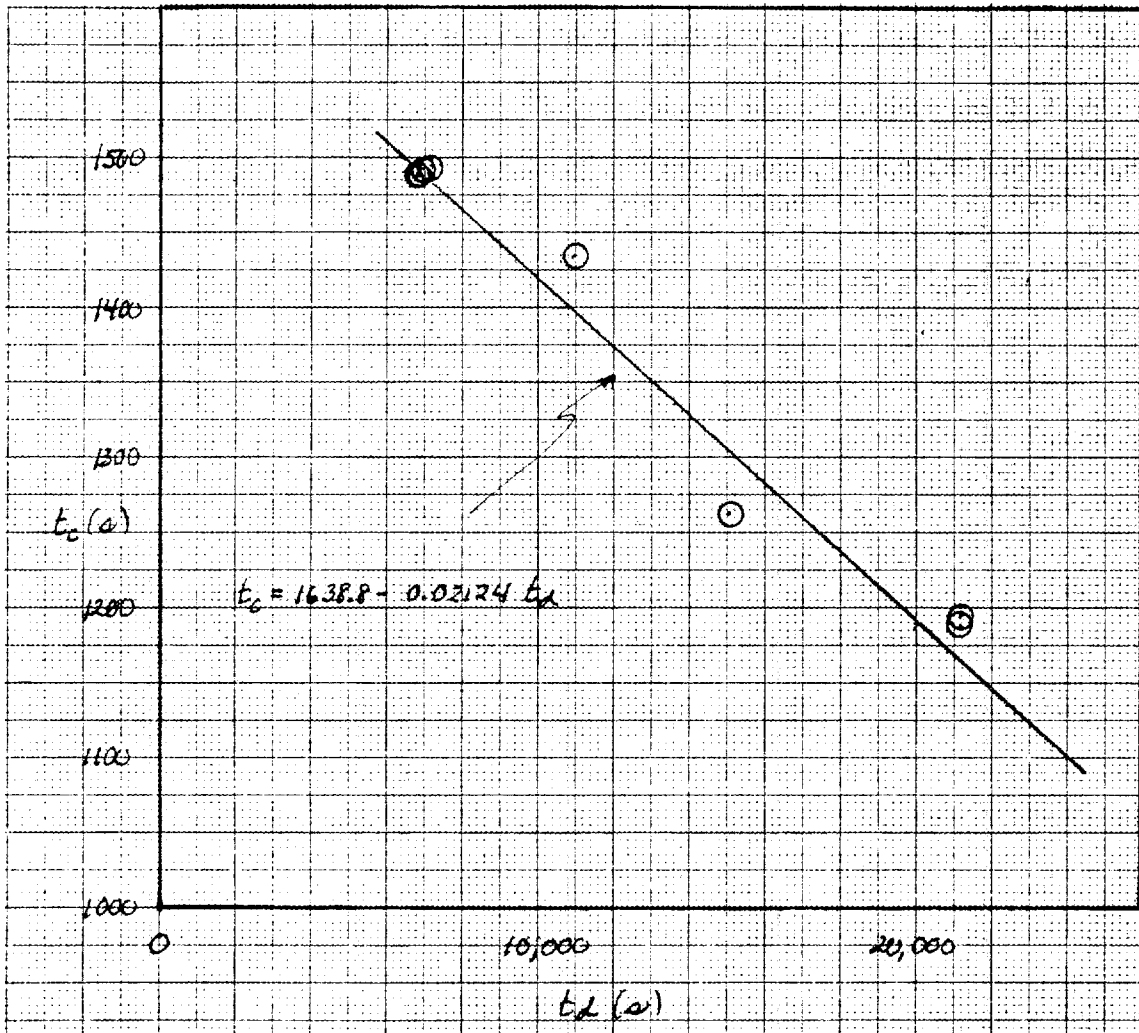


Fig. 8-1. Correlation between t_c and t_d : Used to estimate t_c which was missing for spectrum 2399

[MM-100-WORMM]

9. RAW DATA ON GAMMA COUNTING OF GAS SAMPLES BETWEEN JUNE 10 AND 20
FROM CAPSULE C

The raw data on gamma counting of gas samples between June 10 and 20 from capsule C were given to the author for his personal use only. At the request of R. Conrad, these data are not included in this report. The use of these data was essential in developing several of the sections of this report and their availability is greatly appreciated.

10. QUESTIONS, COMMENTS, AND REQUESTS

1. In reporting the R/B values, it is preferable to use the time of release of the gas sample from the fuel, or the time of collecting the sample, rather than the time at which counting began.
2. On Table 1 of HFR/87/12380, for capsule B, cycle 87.03 at 24.04.87 16.58, the R/B is clearly in error; not only are the R/Bs abnormally high, but the R/B increases with increasing λ , a behavior never observed.
3. In our experience with HRB-17/18, the decline in the fission rate density (fissions/m³ · s) was responsible for a decline in R/B (under nonhydrolyzing and constant temperature conditions). Therefore, we need to know the fission rate density as a function of irradiation time. Do the R/B calculations use a constant fission rate density, in effect, over a cycle, or is the change taken into account?
4. What are the gamma detector efficiencies at 81, 150, 196, 250, and 403 KeV?
5. How is the pulse pileup loss corrected? What are the values of the parameters involved?
6. Relative low values of ⁸⁸Kr are reported (HFR/87/12380). The discussion of this in Section 7 leads to the question of why this occurs in HFR-B1 but not in recent comparable experiments.

7. In reporting the water vapor concentration in ppmv, it is also necessary to give the pressure of the gas at measurement.
8. Can printouts of numerical data corresponding to the graphs in HFR/87/12380 be obtained?
9. The operation of the gas chromatograph, as discussed in Section 5 above, leads to questions about (1) the automatic integration and reporting of concentrations in ppmv (pressure) and (2) the interference by neon. (I see no way other than excluding neon (as suggested in Section 5) for resolving the interference). The results obtained in the second water vapor injection test, when extensive interference by neon occurred, are essentially not useful.
10. I am unable to calculate the relative R/B values for $^{85}\text{m Kr}$, from the ~~raw~~^{raw} data I received when I was at Petten, so as to be in agreement with the reported values. I would very much appreciate help on this matter. (see Sections 2, 6, and 7).
11. The reporting of the gas chromatographic results has yet to be organized. I hope that these results will be available in the detail in which they have been considered in Sections 2 and 5.
12. Before embarking on a long analysis, I need to know a large fraction of the details as I hope this memorandum demonstrates in order to avoid errors in the initial stages which, when later discovered, require much additional work.

Therefore, my inquiries have the objective of my avoiding useless attempts at analysis. Also, my preferred approach to a problem of analysis is to delve in excruciating detail into the problem although I have seldom, if ever, under the HTGR program, been able to satisfy myself on this matter.

DISTRIBUTION

External Distribution

U.S. Department of Energy, Division of HTGRs, Office of Advanced Reactor
Programs, NE531, Washington, D.C. 20545

J. E. Fox

GA Technologies Inc., P. O. Box 85608, San Diego, CA 92138

J. W. Ketterer
F. C. Montgomery
O. M. Stansfield
R. F. Turner

Internal Distribution

D. T. Goodin
M. J. Kania
P. R. Kasten
B. F. Myers